



Contents lists available at ScienceDirect

Tunnelling and Underground Space Technology

journal homepage: www.elsevier.com/locate/tust

A simplified elastic analysis of tunnel-piled structure interaction



Andrea Franza^{a,*}, Alec M. Marshall^a, Twana Haji^a, Amged O. Abdelatif^b, Sandro Carbonari^c, Michele Morici^d

^a Department of Civil Engineering, University of Nottingham, University Park, NG7 2RD Nottingham, United Kingdom

^b Department of Civil Engineering, University of Khartoum, P.O. Box 321, 11111 Khartoum, Sudan

^c DICEA, Università Politecnica delle Marche, Via Brecce Bianche, 60131 Ancona, Italy

^d SAAD, University of Camerino, Viale della Rimembranza, 63100 Ascoli Piceno, Italy

ARTICLE INFO

Article history:

Received 4 April 2016

Received in revised form 10 August 2016

Accepted 16 September 2016

Available online 18 October 2016

Keywords:

Tunnelling

Pile

Soil-structure interaction

Building response

ABSTRACT

In urban areas, engineers often need to assess tunnelling-induced displacements of piled structures and the resulting potential for damage. This paper presents an elastic study of tunnel-pile-structure interaction through Winkler-based Two-Stage Analysis Methods (TSAMs), focusing on structural displacements resulting from tunnel excavation beneath piled frames or simple equivalent beams. Comparison of results with 3D finite element analyses shows that the simple TSAM models are able to provide a good assessment of tunnelling-induced building displacements. Parametric analyses highlight the role of tunnel-pile interaction and the superstructure (stiffness, configuration, and pile-structure connections) in the global response of the tunnel-soil-building system. In particular, the effect that key parameters have on deflection ratios and horizontal strains are investigated. Results illustrate how piled foundations increase the risk of structural damage compared to shallow foundations, whereas structural stiffness can reduce building deformations. Flexural deformations are predominately induced by tunnel excavations beneath piles whereas horizontal strains at the ground level are negligible when a continuous foundation is included. Furthermore, it is illustrated that results based on buildings modelled as equivalent beams can differ considerably compared to when they are modelled as framed structures. Simple design charts are provided to estimate horizontal strains and deflection ratio modification factors based on newly defined relative axial and bending stiffness parameters which account for the presence of the piles.

© 2016 The Authors. Published by Elsevier Ltd. This is an open access article under the CC BY license (<http://creativecommons.org/licenses/by/4.0/>).

1. Introduction

In urban areas, the increasing demand for infrastructure and development of services has resulted in tunnel construction and deep excavations taking place in close proximity to buried infrastructure and building foundations. To avoid possible damage to structures, engineers need to be able to accurately assess excavation-induced deformations of the buildings. However, although various studies have considered the effect of excavations on either a building with shallow foundations or piles connected by a rigid cap, the understanding of how the tunnel-pile interaction affects the response of buildings is still not well understood.

Various studies have considered the case of tunnel construction beneath buildings with shallow foundations. It has been recognised that the building stiffness should be taken into account in the assessment of tunnel-structure interaction since it generally

tends to decrease the structural distortions and risk of damage with respect to the greenfield case (Franzius et al., 2006; Dimmock and Mair, 2008; Maleki et al., 2011; Farrell et al., 2014; Giardina et al., 2015). On the other hand, the tunnel-single pile and pile group interaction problems have been widely analysed using field trials, physical modelling, and numerical simulations, leading to some confidence in the assessment of pile group displacements (Jacobsz et al., 2004; Kaalberg et al., 2005; Selemetas, 2005; Devriendt and Williamson, 2011; Marshall and Mair, 2011; Dias and Bezuijen, 2015), internal forces (Kitiyodom et al., 2005; Huang et al., 2009; Ng et al., 2012; Soomro et al., 2015), and pile failure due to tunnel excavation (Marshall and Haji, 2015). However, as indicated by Mair and Williamson (2014), studies have focused predominately on tunnelling adjacent to piles, for which the induced building distortions are expected to be minimal. In these cases, tunnelling mainly causes lateral bending in piles rather than settlements along the pile axis. In contrast, tunnelling beneath piles induces vertical pile movements, which leads to structural deformations. Moreover, it is important to note that only

* Corresponding author.

E-mail address: andreafranza@gmail.com (A. Franza).

a few studies have considered the effects of structural configuration on building deformations induced by excavations. Goh and Mair (2014) highlighted the importance of structural configuration in the global interaction based on an extensive set of numerical analyses which evaluated the response of framed buildings to deep excavations. Fagnoli et al. (2015) suggested that the use of an equivalent plate and beam model for the superstructure may lead to an erroneous evaluation of the structural response to tunnelling-induced movements. The work of Losacco et al. (2014) suggested that, in order to obtain satisfactory results, more advanced simplified structural models of the building, rather than a simple beam/plate, could be incorporated into the global interaction analysis.

In a preliminary risk assessment of building damage caused by tunnelling, it is important to be able to predict, with reasonable simplicity and reliability, the induced structural deformations. However, for tunnelling beneath buildings on piled foundations, there is a limited amount of information and guidance available to inform such a risk assessment. In practice, engineers typically evaluate the tunnelling-induced deformations empirically, assuming that pile heads settle according to a subsurface greenfield settlement profile. The depth of the selected settlement trough is usually taken at some distance between the surface and the pile tip in order to account for the piles being dragged down by subsurface soil movements (Devriendt and Williamson, 2011). For tunnels, several relationships between surface greenfield soil displacements and pile head settlements have been proposed depending on pile tip position. For instance, Kaalberg et al. (2005) and Selemetas (2005) suggested three zones where pile head settlements may be larger than (zone A), equal to (zone B) or smaller than (zone C) the greenfield surface settlements (see Fig. 1). These also agree qualitatively with results obtained by other researchers who used centrifuge testing to study the problem (Jacobsz et al., 2004; Marshall and Mair, 2011).

However, despite the general agreement, a comparison of previous studies carried out by Dias and Bezuijen (2015) demonstrated that the relationship between pile head and greenfield surface settlements is not a unique function of the relative tunnel-pile tip position; it also depends on working loads, tunnel volume loss, and distribution of working load between pile base and shaft. As shown in Fig. 2, Dias and Bezuijen (2015) indicated that the regions A-B-C defining the relative pile/surface settlements do not capture the full complexity of the problem. The authors suggested an upper limit of the normalised pile head settlement depending on the normalised horizontal pile offset to the tunnel centreline. However, use of this upper limit would lead to an over-conservative assessment of tunnelling-induced deformation in piled buildings.

The previous studies indicate that piles with their tips directly above the tunnel (i.e. within a horizontal offset of one tunnel

radius from the tunnel axis) are likely to settle more than the surface, whereas piles outside this area generally settle less than the surface. This causes a narrowing of the pile head settlement profile with respect to the greenfield surface settlement trough, leading to an increased potential for building damage. Moreover, assessing tunnelling-induced deformations in buildings using a tunnel-pile interaction analysis (i.e. assuming that the building follows the settlement curve obtained from a tunnel-pile or tunnel-pile group analysis) does not allow inclusion of the influence of the building on the global interaction; this may be overly conservative in the cases of relatively stiff structures, as illustrated by a case study reported by Goh and Mair (2014).

In the first part of this paper, the complete tunnel-pile-structure interaction is investigated through a Winkler-based Two-Stage Analysis Method (TSAM), focusing on structural displacements that result from the tunnel excavation. Since displacements are damage related quantities, their prediction can be used to evaluate building serviceability state. The TSAM method is able to capture the main interaction mechanisms and the effects of structural configuration on the global response of the system to tunnelling. In the second part of the paper, effects of structure stiffness on the building deformations, both axial and flexural, are investigated, with emphasis on the role played by the piled foundations. Two simple design charts for evaluating the piled building deflection ratios and horizontal strains are proposed.

2. Background

2.1. Two-stage analysis method (TSAM)

Soil-structure interaction systems are characteristically complex due to the effects of interfaces, soil non-linearity, and plasticity. However, despite this, simplified elastic methods are common in structural and geotechnical engineering. In particular, many useful tools for tunnel-pile interaction analysis have been developed using the elastic framework. These are based on a two-stage procedure: (1) the greenfield soil displacements caused by tunnel excavation are estimated analytically, through closed-form expressions (Loganathan and Poulos, 1998; González and Sagaseta, 2001; Franza and Marshall, 2015), or numerically using software based on the finite element (FE) or finite difference (FD) methods; (2) the analysis of the full system, including soil, foundation and superstructure, is carried out considering the foundation subjected to a system of external loads that would, in the absence of the included structure, reproduce the greenfield soil movements.

Two-staged analyses of tunnel-pile interaction problems have incorporated continuum or Winkler-based analyses in order to study tunnel-single pile and tunnel-pile group interactions. Chen et al. (1999) and Loganathan et al. (2001) used a boundary element method (BEM) to analyse pile groups. Basile (2014) extended previous works to include the non-linear soil behaviour within the BEM. The main conclusion of previous works is that the group effect is beneficial, resulting in a reduction of foundation displacements and internal pile forces compared to isolated piles. Moreover, the work of Basile (2014) indicated that soil non-linearity leads to a remarkable reduction of axial forces within the piles. Kitiyodom et al. (2005) and Huang et al. (2009) considered a beam on a Winkler elastic foundation to study the problem of tunnel-pile group interaction, confirming the beneficial effects of pile-soil-pile interaction. Zhang et al. (2011a,b) and Zhang et al. (2013) improved the soil model to account for soil nonlinearities and pile-soil interface characteristics in order to assess the influence of working loads. It was shown that existing working loads have an influence on the pile-tunnel interaction; the increase of pile working loads results in an increase of excavation-induced pile

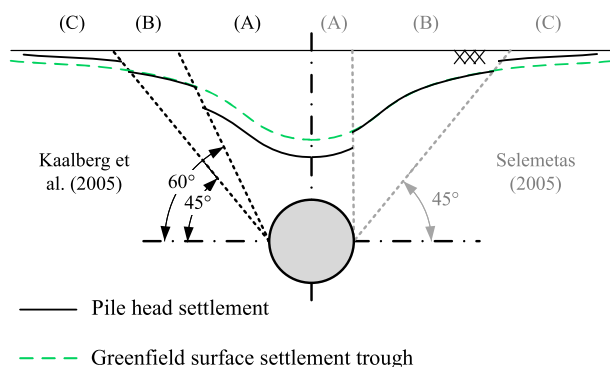


Fig. 1. Proposed relationships between pile head and greenfield surface settlements depending on pile tip location.

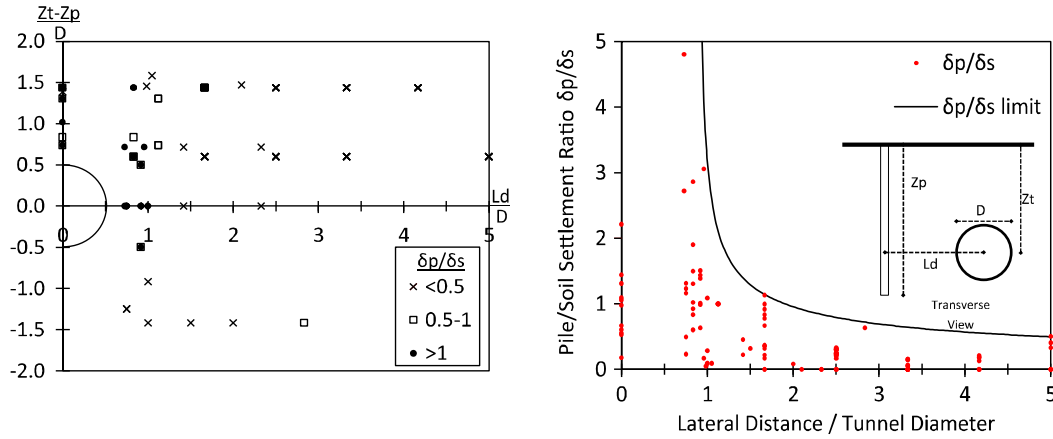


Fig. 2. Analysis of pile settlement data: (a) ratio between the pile (δp) and the ground surface settlements (δs) with respect to the pile tip position; (b) upper envelope of measured $\delta p/\delta s$ at different normalised lateral distances (Dias and Bezuijen, 2015).

settlements and a decrease of tunnelling effects on axial forces within the piles.

Recent studies have shown that the assumptions of soil linear-elasticity and perfect bonding between the soil and pile provide good predictions over the range of tunnel ground losses typically experienced in practice (i.e. $V_{lt} = 0.5\text{--}1\%$), whereas non-linearity and plasticity play a more important role at higher volume losses (Zhang et al., 2011a, 2013; Basile, 2014). Moreover, centrifuge tests have indicated a decrease of structural damage induced by tunnelling in elastic buildings with shallow foundations as tunnel volume loss increases because of the soil stiffness degradation (Farrell et al., 2014). Therefore, a fully elastic analysis appears to be adequate to highlight the main interaction mechanisms; moreover, it provides insight to help understand the global tunnel-piled building interaction, as long as tunnel ground loss does not induce pile failure.

2.2. The modification factor approach and relative stiffness factors

The building modification factor approach was introduced by Potts and Addenbrooke (1997) to relate building deformations (maximum deflection ratio, DR , and maximum horizontal strain, ε_h) caused by adjacent excavation and tunnelling activities to surface greenfield soil movements.

The deflection ratio modification factor, M^{DR} , is calculated by dividing the building sagging and hogging deflection ratio resulting from tunnel construction ($DR_{sag,Bldg}$; $DR_{hog,Bldg}$) by the deflection ratio of the greenfield settlement trough ($DR_{sag,GF}$; $DR_{hog,GF}$), as shown in Fig. 3.

$$M^{DR,sag} = \frac{DR_{sag,Bldg}}{DR_{sag,GF}} \quad \parallel \quad M^{DR,hog} = \frac{DR_{hog,Bldg}}{DR_{hog,GF}} \quad [-] \quad (1)$$

The modification factors for the maximum tensile and compressive horizontal strains, $M^{eh,t}$ and $M^{eh,c}$, are given by the ratio between the maximum building strains ($\varepsilon_{h,t,Bldg}$; $\varepsilon_{h,c,Bldg}$) and the maximum greenfield horizontal strains at the building location ($\varepsilon_{h,t,GF}$; $\varepsilon_{h,c,GF}$).

$$M^{eh,t} = \frac{\varepsilon_{h,t,Bldg}}{\varepsilon_{h,t,GF}} \quad \parallel \quad M^{eh,c} = \frac{\varepsilon_{h,c,Bldg}}{\varepsilon_{h,c,GF}} \quad [-] \quad (2)$$

Evaluation of the deflection ratio and the horizontal strains at the foundation level represents the first step towards a preliminary building damage assessment based on the limiting tensile strain method. For the sake of simplicity, a building that spans hogging

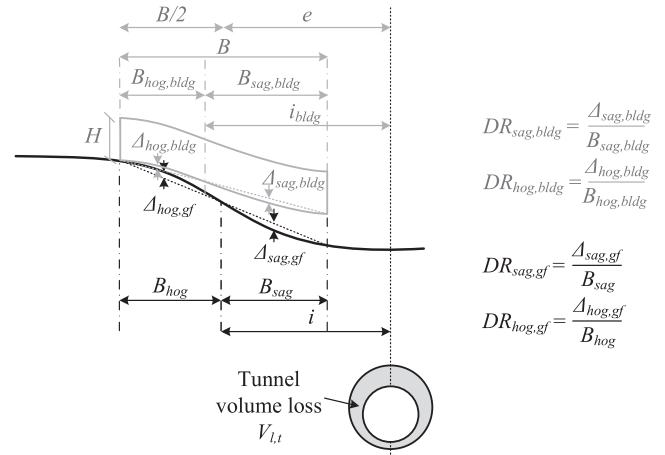


Fig. 3. Definition of relative deflection, Δ , and deflection ratio, DR , in sagging and hogging.

and sagging zones is commonly considered as two independent structures. Subsequently, the damage assessment in hogging and/or sagging is performed by comparing maximum building tensile strain with a limiting tensile strain (Mair et al., 1996).

2.2.1. Simple beam and plate structures

Several relative stiffness factors (i.e. the stiffness of the structure in relation to that of the soil) have been proposed to assess the contribution of structural stiffness in reducing the damage induced by greenfield ground movements. The use of relative stiffness factors was proposed by Potts and Addenbrooke (1997) and later modified to a dimensionless form by Franzus et al. (2006). These authors carried out parametric finite element analyses of building deformations caused by tunnelling and showed that the resulting building deflection is mostly dependent on relative bending stiffness, whereas final building axial strains depend on relative axial stiffness. They summarised their results in design charts in which reduction factors are related to the appropriate relative stiffness, depending on deformation zone (sagging, hogging) and the ratio e/B , where eccentricity e is the horizontal distance from the tunnel centreline to the centre of the building with width B in the transverse direction (illustrated in Fig. 3). The dimensionless forms of the relative bending stiffness, ρ_{mod}^* , and the relative axial stiffness, α_{mod}^* , are given by

$$\rho_{mod}^* = \frac{EI}{E_s z_t B^2 L} \quad \parallel \quad \alpha_{mod}^* = \frac{EA}{E_s BL} \quad [-] \quad (3)$$

where EI and EA are the bending and axial stiffness of the superstructure (in kN m^2 and kN), respectively, E_s is the soil Young's modulus that may be estimated as the secant stiffness of the soil at an axial strain of 0.01% and at a depth of $z = z_t/2$, z_t is the tunnel axis depth, and L is the longitudinal length of the building.

To generalise the design charts suggested by [Franzius et al. \(2006\)](#) and reduce the level of scatter, [Farrell \(2010\)](#) and [Goh and Mair \(2011\)](#) proposed the following dimensionless expressions for the relative bending stiffness in sagging and hogging zones that account indirectly for the tunnel-building eccentricity:

$$\rho_{sag} = \frac{EI}{E_s B_{sag}^3 L} = \frac{(EI)^*}{E_s B_{sag}^3} \quad \parallel \quad \rho_{hog} = \frac{EI}{E_s B_{hog}^3 L} = \frac{(EI)^*}{E_s B_{hog}^3} \quad [-] \quad (4)$$

where $(EI)^*$ is the bending stiffness of the building per running metre (in $\text{kN m}^2/\text{m}$ run), and B_{sag} , B_{hog} are the lengths of the building in the sagging and hogging zones based on the greenfield settlement trough (i.e. for a fully flexible building). The authors suggested that a representative value for soil stiffness could be based on a weighted average of the elastic modulus of the soil above the tunnel at a level of strain that is representative of the tunnelling scenario. The soil and building stiffnesses are difficult parameters to evaluate accurately, however a reasonable assessment of the modification factors only requires determination of relative stiffness within an order of magnitude because of the semi-logarithmic scale of design charts ([Mair, 2013](#)). This definition of relative bending stiffness permitted [Mair \(2013\)](#) to describe, with narrow envelopes, data of M^{DR} obtained for tunnelling and deep excavations from finite element analyses, centrifuge modelling and field studies available in the literature.

2.2.2. Deflection ratio for framed buildings

For framed structures, several authors have discussed the possibility of simplifying the interaction analysis by considering an equivalent simple beam or plate. To estimate the bending stiffness of the equivalent beam, [Potts and Addenbrooke \(1997\)](#) suggested the use of the parallel axis theorem, whereas [Mair and Taylor \(2001\)](#), neglecting the stiffening effect of shear walls, connections, and columns, indicated that the equivalent bending stiffness should be the algebraic sum of all floor slabs. Although the use of the parallel axis theorem with the corrections proposed by [Dimmock and Mair \(2008\)](#) may be appropriate for masonry buildings, both approaches are not adequate in the case of framed structures ([Goh and Mair, 2014](#)). In particular, the use of the parallel axis theorem and the algebraic sum provide an overestimation and underestimation of the overall structural stiffness, respectively.

In the case of frame structures, it is necessary to correctly account for the stiffening contribution of columns to the beam flexural stiffnesses. If bays have an approximately equal length, [Goh and Mair \(2014\)](#) showed that this effect may be estimated with the following column stiffening factor, obtained from the structural analysis of a frame deflecting in a sagging deformation mode:

$$C_{sag} = \left[1 + \frac{B_{sag}^2}{l^2} \left(\frac{K_{LC} + K_{UC}}{K_{LC} + K_{UC} + K_B} \right) \right] \quad (5)$$

$$C_{hog} = \left[1 + \frac{B_{hog}^2}{l^2} \left(\frac{K_{LC} + K_{UC}}{K_{LC} + K_{UC} + K_B} \right) \right]$$

where l is the span length of each beam bay, h is the storey height, $K_{LC} = (EI/h)_{LC}$ is the average stiffness of the lower column, $K_{UC} = (EI/h)_{UC}$ is the average stiffness of the upper column, and $K_B = (EI/l)_B$ is the average stiffness of the beam line. For [Goh and](#)

[Mair \(2014\)](#), the equivalent bending stiffness of the frame structure is given by

$$EI_{eq,sag} = \sum (C_{sag} * EI)_{floors} \quad \parallel \quad EI_{eq,hog} = \sum (C_{hog} * EI)_{floors} \quad (6)$$

It is important to note that C depends on the number of spans in the hogging or sagging zones, B_{sag}/l or B_{hog}/l ; the coefficient C increases with the number of spans because of the contribution of additional columns to the stiffness of the beams. With reference to deflection ratio modification factors, the effectiveness of Eq. (6) was shown for framed structures subjected to deep excavation-induced movements. However, further investigation is needed for the case where piled foundations are included.

2.2.3. Horizontal strains in framed buildings

For shallow foundations, [Goh and Mair \(2014\)](#) derived a stiffness parameter that is able to approximately quantify the contribution of the frame to the reduction of horizontal strains compared to greenfield soil movements. The reaction of the structure at the ground level to horizontal strains was conservatively estimated considering a simple portal frame with a single bay on two pin-supports. The frame stiffness factor α_f was defined by imposing a unit differential horizontal displacement Δ between the pin-supports and calculating the external horizontal reaction force H . The stiffness parameter is a function of $K_c = EI_c/h$ and $K_b = EI_b/l$, where h is the column height, EI_c and EI_b are the bending stiffness of the column and the first-floor beam, respectively. This stiffness parameter, α_f , is not dimensionless. As recognised by [Goh and Mair \(2014\)](#), a single portal neglects the influences of additional storeys, variable bay length, and the presence of structural infill walls with bearing capacity. The following expression was used by [Goh and Mair \(2014\)](#) to define a reasonable upper bound for α_f :

$$\alpha_f = \frac{H}{\Delta} = \frac{3K_b K_c}{h^2 (2K_b + 3K_c)} \quad [\text{KN/m}] \quad (7)$$

3. Two-stage Winkler-based methods for the analysis of tunnel-piled structure interaction

This section presents details of the TSAMs used in this paper. Two tunnel-pile-structure interaction (TPSI) approaches were adopted: a general method (Method G, referred to as TPSI-G) proposed by [Kitiyodom et al. \(2005\)](#), based on deformable interacting piles, and a simplified version (Method S, referred to as TPSI-S), based on the assumption of rigid isolated piles. The simplified Method S, described in [Franza et al. \(2016\)](#), provides a relatively easy way to calculate tunnelling-induced settlements of piled buildings which may be useful when conducting preliminary risk assessments. A schematic representation of the two methods is shown in [Fig. 4](#).

The analysis is limited to two structural cases: either an elastic frame structure or a simple equivalent beam. The structures are supported by a foundation consisting of a row of uniformly spaced circular piles embedded vertically in an elastic homogeneous deposit. The foundation and structure are affected by displacements caused by the construction of a tunnel beneath the level of the pile tips. The structure is orthogonal to the longitudinal tunnel axis and is not in contact with the ground surface. Tunnelling induces vertical and lateral ground movements that cause displacements in the foundation-superstructure system. Note that this is not a plane strain problem because both the foundation and structure have a finite length in the tunnel longitudinal direction. It should be noted that the building weight was not considered in the paper because, under the assumptions of the

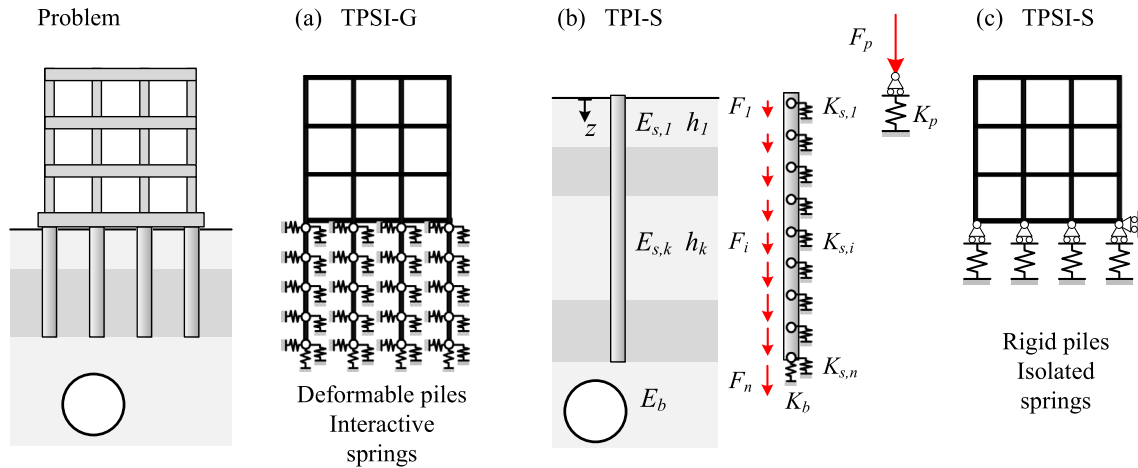


Fig. 4. Winkler model for tunnel-pile-structure interaction (TPSI): (a) deformable piles and interactive springs (method G); (b) single rigid pile (method S); (c) isolated rigid piles (method S).

proposed analysis method, the displacements induced by tunnelling and building self-weight would not affect each other.

3.1. Greenfield displacement input

The prediction of tunnelling-induced soil movements may be performed with empirical, finite element, or analytical methods. Empirical methods have been used extensively in practice for the estimation of settlement trough shape because of their inherent simplicity. Empirical methods, however, do not provide reliable predictions of horizontal movements throughout the soil depth. On the other hand, finite element analyses generally require significant computational effort and detailed soil constitutive model input data that may not be available. Closed-form analytical and semi-analytical solutions have been successfully adopted in tunnel-soil-structure interaction analyses, especially when horizontal ground displacements are important (e.g. tunnel-pile interaction analyses), because they provide a consistent deformation pattern with depth. The closed-form expressions proposed by Loganathan and Poulos (1998) for the prediction of vertical and horizontal greenfield tunnelling-induced displacements in clays were adopted for the analyses presented in this paper. However, any greenfield displacement input could be used within the proposed method, thereby enhancing the versatility of the approach.

3.2. Soil springs

In this paper, the soil-pile interaction problem is modelled through vertical and horizontal linear springs distributed along the pile shaft, and by means of a vertical spring placed at the pile base; slippage and gap formation are not allowed. Several methods are available in the literature for evaluating spring stiffness. For piles subjected to passive loads due to ground movements, Kitiyodom et al. (2005) demonstrated that the integral method is most suitable when the estimation of pile internal forces, in particular axial forces, is important. However, in this study, for the sake of simplicity, the horizontal and vertical soil spring stiffness were correlated to the elastic parameters of the soil with the expressions suggested by Vesic (1961) and Randolph and Wroth (1978). As shown by Mylonakis and Gazetas (1998) and Huang et al. (2009), these expressions allow for a good estimation of the displacements of floating piles induced by tunnelling and external loadings at the pile heads, which are of great importance for correctly describing tunnel-piled building interaction.

The assumed values of stiffness for vertical (k_z) and horizontal (k_x) shaft springs (per unit-length of pile) are given in Eq. (8).

$$k_z = \frac{2\pi G_s}{\ln\left(\frac{2r_m}{d_p}\right)} \quad \parallel \quad k_x = \frac{0.65E_s}{d_p(1-\nu_s^2)} \sqrt[12]{\frac{d_p^4 E_s}{E_p I_p}} \quad (8)$$

where G_s is the shear modulus of soil, E_s and ν_s are the Young's modulus and Poisson's ratio, respectively, of the soil at the pile shaft, r_m is an empirically determined distance beyond which the soil settlements become negligible, d_p is the pile diameter, L_p is the pile length, and $E_p I_p$ is the flexural pile stiffness. In general, $r_m = \chi_1 \chi_2 L_p (1 - \nu_s)$ where χ_1 and χ_2 are empirical terms depending on soil inhomogeneity ($\chi_1 \chi_2 = 2.5$ in the case of a homogeneous half-space) (Randolph and Wroth, 1978; Mylonakis and Gazetas, 1998). The stiffness of the vertical spring K_b^p at the pile base is evaluated with Eq. (9) (Randolph and Wroth, 1979),

$$K_b^p = \frac{d_p E_b}{1 - \nu_b^2} \quad (9)$$

where E_b and ν_b are the Young's modulus and Poisson's ratio, respectively, of the soil below the pile base.

3.3. General analysis method for tunnel-pile-structure interaction

The 'General Method' of tunnel-pile-structure interaction (TPSI) analysis (referred to as TPSI-G, refer to Fig. 4) used in this paper was achieved numerically by means of the finite element method (FEM) using a displacement-based approach. Using this method, when matrix condensation is conducted for the structure with respect to the pile head nodes, the remaining degrees of freedom (dofs) of the system are the generalised displacements of the pile element nodes (i.e. vertical and horizontal displacements, and rotations). Condensation of the problem allows reduction of the dofs (i.e. the computational effort of the analysis) while preserving the rigour of the approach. The equilibrium condition of the soil-pile-structure system is expressed by the following system of linear equations:

$$(\mathbf{C} + \mathbf{K}_s + \mathbf{K}_p) \mathbf{u}_p = \mathbf{f}_p \quad (10)$$

where $(\mathbf{C} + \mathbf{K}_s + \mathbf{K}_p)$ is the global stiffness of the piled structure system, \mathbf{C} is the soil stiffness matrix, \mathbf{K}_s is the condensed stiffness matrix of the structure, \mathbf{K}_p is the stiffness matrix of the pile group, and \mathbf{u}_p is the displacement vector of the piled foundation. Note that $\mathbf{f}_p = \mathbf{C}\mathbf{s}$ represents the external force vector acting on the piles due

to vertical and lateral tunnelling-induced greenfield ground movements, where \mathbf{s} is the vector of the tunnelling-induced greenfield movements. Eq. (10) may be partitioned to highlight the dofs of the pile heads connected to the superstructure (subscript F) and of the embedded pile nodes (subscript E):

$$\left[\begin{array}{cc} \mathbf{C}_{FF} & \mathbf{C}_{FE} \\ \mathbf{C}_{EF} & \mathbf{C}_{EE} \end{array} \right] + \left[\begin{array}{cc} \mathbf{K}_{FF} & \mathbf{0} \\ \mathbf{0} & \mathbf{0} \end{array} \right]_s + \left[\begin{array}{cc} \mathbf{K}_{FF} & \mathbf{K}_{FE} \\ \mathbf{K}_{EF} & \mathbf{K}_{EE} \end{array} \right]_p \begin{bmatrix} \mathbf{u}_F \\ \mathbf{u}_E \end{bmatrix}_p = \begin{bmatrix} \mathbf{C}_{FF} & \mathbf{C}_{FE} \\ \mathbf{C}_{EF} & \mathbf{C}_{EE} \end{bmatrix} \begin{bmatrix} \mathbf{s}_F \\ \mathbf{s}_E \end{bmatrix} \quad (11)$$

Piles and superstructure elements are modelled as Euler-Bernoulli elastic beams. The soil stiffness matrix is defined as $\mathbf{C} = \mathbf{A}^{-1}$, where \mathbf{A} is the soil flexibility matrix whose generic components A_{ij} describe soil displacement at node i of the pile induced by a unit force applied at node j . In this analysis, the interaction between nodes belonging to the same pile was neglected as well as the interaction between shaft and base nodes (i.e. pile base nodes only interact with each other). The diagonal terms of the flexibility matrix were determined starting from the stiffness values obtained by Eqs. (8) and (9). In this paper, the analyses were limited to the case of a homogeneous half-space, thus the off-diagonal non-zero terms, which represent pile-soil-pile interaction contributions, were obtained on the basis of Mindlin (1936) solutions for vertical and lateral forces at the pile shaft. Concerning displacements induced at a radial distance r by vertical forces at the pile base, the off-diagonal terms were obtained from the approximate attenuation function of soil settlements, $d_p/(\pi r)$, suggested by Randolph and Wroth (1979), which was derived from the solution of a punch on the surface of a half-space.

Once the equilibrium equation is solved with the inverse matrix method, the solution displacement vector, \mathbf{u}_p , is obtained. Then, the displacements and deformations of the entire superstructure can be computed by displacing the dofs of the pile heads connected to the superstructure by the sub-vector \mathbf{u}_F . Subsequently, superstructure internal forces and bending moments may be computed.

3.4. Simplified analysis method for tunnel-pile-structure interaction

The ‘Simplified Method’ for tunnel-pile-structure interaction analysis (referred to as TPSI-S) used in this paper (1) assumes the piles to be rigid, (2) neglects the pile-soil-pile interaction, and (3) disregards the horizontal soil springs. Subsequently, this procedure only requires consideration of the vertical dofs of the piles. These simplifying assumptions reduce the global tunnel-pile-structure interaction analysis to that of a building on vertical springs which account for the soil deformability, subjected to a vertical system of forces induced by tunnelling (Fig. 4(c)).

The schematic representation of the problem for a single pile case is shown in Fig. 4(b). If each pile is discretised into $n + 1$ nodes, it is possible to provide the following simple closed-form expressions for the stiffness of the equivalent pile-soil spring, K_p , and the resultant tunnelling-induced vertical force, F_p , at the p th pile head.

$$K_p = \sum_{i=1}^n k_z(z_i) \Delta z_i + K_b^p \quad (12)$$

$$F_p = \sum_{i=1}^n s_z(z_i) k_z(z_i) \Delta z_i + s_z(L_p) K_b^p$$

where Δz_i is the effective pile length corresponding to the i th node, and s_z is the greenfield vertical soil movement induced by tunnel excavation at the p th pile axis line.

If a piled structure is considered, the tunnel excavation induces a system of vertical forces at the pile head level. The equilibrium equation of the system is formulated by adding the contribution

of soil stiffness to the condensed stiffness matrix of the structure. The equilibrium equation is

$$(\mathbf{K}_s + \mathbf{K}_g) \mathbf{u}_p = \mathbf{f}_p \quad (13)$$

where \mathbf{K}_s is the condensed stiffness matrix of the structure, \mathbf{K}_g is the stiffness matrix of the soil-pile group system, \mathbf{u}_p is the displacement vector of the piled foundation, and \mathbf{f}_p is the vector of the tunnelling-induced forces. The condensed stiffness matrix of the structure is a full matrix, whereas the stiffness matrix of the pile-soil system is a diagonal matrix because the pile-soil-pile interaction is neglected. The non-zero diagonal terms of $K_{g,i,i}$ and the terms of vector $f_{p,i}$ are obtained from Eq. (12). Note that, because the problem is idealised as an elastic structure on independent vertical elastic springs, the superstructure should be restrained in the horizontal direction by an additional external constraint (see Fig. 4(c)). Neglecting horizontal ground movements at the pile foundation is acceptable considering that tunnel construction generally induces negligible horizontal strains in structures with continuous foundation systems at the ground level (due to the relatively high axial stiffness of the building/foundation system) (Burland et al., 2004; Dimmock and Mair, 2008). However, this may not be the case for isolated piles or a foundation with a particularly low axial stiffness at the ground level (e.g. single columns supported by a single pile not connected at the ground floor level) (Goh and Mair, 2014). In these cases, particular attention should be paid in using the outcomes of the simplified Method S. In the analysis presented here, solution to Eq. (13) was obtained with the inverse matrix method. Alternatively, a 3D numerical modelling software could be used. Although results presented here are limited to a simple pile row foundation, this analysis method can account for layered soil deposits and a generic structure with a variety of pile foundation configurations.

4. Model validation

This section demonstrates that the Winkler-based methods allow for a reliable assessment of piled building displacements due to tunnel construction. The efficacy of Methods G and S was investigated by comparing results against more rigorous 3D elastic FEM analyses performed using ABAQUS (Simulia, 2010). The influence of tunnel location, building configuration, as well as soil and structure stiffness were investigated. Although the analytical models allow implementation of multi-layered soil, all considered configurations correspond to vertical piles embedded in a homogeneous half-space. Results focus on the tunnelling-induced structural distortions at the foundation level (i.e. pile head movements). Pile head vertical and horizontal displacements are indicated as u_z^p and u_x^p , respectively, whereas rotations are given by φ^p . Tunnel-pile group interaction performed with free-pile head conditions (i.e. piles are not affected by a structure) are indicated with TPI; tunnel-pile-structure interaction analyses are denoted with TPSI. Fig. 5 summarises the considered tunnel-pile-structure configurations and illustrates the adopted sign convention for displacements and rotations.

Before performing the validation analyses, a sensitivity study was performed to estimate the influence of pile finite element size on translations and rotations of the pile heads obtained with method G. Results showed that, for the considered frame case, the convergence was easily reached with an element size, Δh , smaller than $2.5 d_p$. In the model validation section, a finite element size $\Delta h = 0.5$ m was adopted. In later sections, when not stated, $\Delta h = 1.0$ m was used because it resulted in a reliable and computationally efficient analysis.

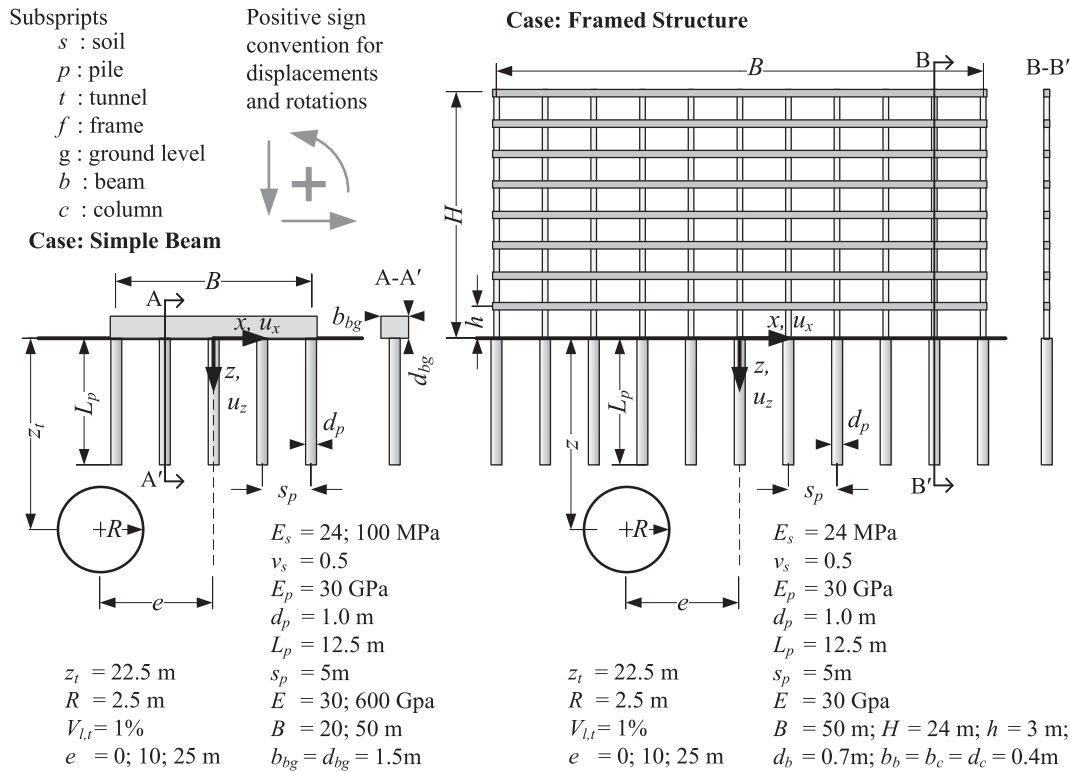


Fig. 5. Studied configurations for the validation.

4.1. Definition of analysis cases

Validation analyses were performed with for two structural/foundation models: (1) simple beams with a foundation comprising a row of either 5 or 11 piles, and (2) a framed structure with an 11 pile foundation, each of which was supported by a pile, and with no ground-level beam connecting the columns. The simple beam was given a stiffness that is representative of an equivalent foundation and superstructure system. Several relative soil-structure stiffness ratios, given by E_s/E , where E_s and E are the Young's modulus of the soil and superstructure, respectively, were investigated. The framed structure elements were given a Young's modulus of 30 GPa and realistic beam and columns cross-sections (as detailed in Fig. 5). The pile spacing was fixed at 5 m, hence the 5-pile building model had a width $B = 20$ m, whereas the 11-pile foundation had a width $B = 50$ m. The structures were located with their centre at a horizontal distance e from the tunnel centreline. Three different tunnel locations, $e = 0, 15$, or 25 m, were considered. The tunnel volume loss, $V_{l,t}$, was assumed equal to 1% for all the performed analyses in this paper. In this section, piles were assumed to be constrained through fixed connections to the superstructure. Both horizontal and vertical greenfield movements were considered except for the simple beam case, where only tunnelling-induced forces due to vertical greenfield movements were applied.

4.2. ABAQUS finite element models

The validation results were obtained with rigorous 3D elastic FEM analyses performed using ABAQUS. The model was composed of 3D structural bodies (beams and piles) as well as by a 3D soil mesh. Therefore, it correctly models the global interaction under the assumption of linear isotropic materials. The ABAQUS simulations modelled the soil and piles using 3D 8-node linear brick, reduced integration solid elements (C3D8R). The mixed

analytical-numerical approach for soil-structure interaction analysis used by Klar and Marshall (2008) was adopted. This ensured that the input soil displacements due to tunnelling in the numerical model were consistent with those used in the Winkler-based model.

The mixed analytical-numerical analysis consists of two stages. In the first stage, all nodes of the soil model are forced to displace according to a chosen input for greenfield settlements and the reaction forces of the nodes (nodal forces required to produce the applied displacements) are recorded. In the second stage, the model is returned to its original condition (before deformation) and the selected structure is added to the model. The nodal reaction forces recorded in the previous stage are then applied to the model which includes the added structure. Any difference in soil displacements between the two stages of the model is due to the existence of the added structure (piles and superstructure). All other aspects of the ABAQUS model were consistent with the assumptions adopted in the Winkler-based model; tie connections at soil-pile interfaces, linear elastic isotropic materials, no contact between the soil and superstructure, and weightless materials. Furthermore, the model dimensions were set to ensure that boundary conditions did not affect results.

4.3. Validation test results

4.3.1. Simple beam model

A comparison of the ABAQUS and Winkler-based model results for the simple beam analyses are presented in Fig. 6 for different values of soil and equivalent structure stiffness, as well as building location. For comparison, greenfield ground movements (at the surface) are also plotted (see black dashed lines).

Fig. 6 shows that the results obtained with method G match the ABAQUS results; method S gives a good and generally slightly conservative assessment of the tunnelling-induced deformation profile. The difference between the ABAQUS and Winkler model

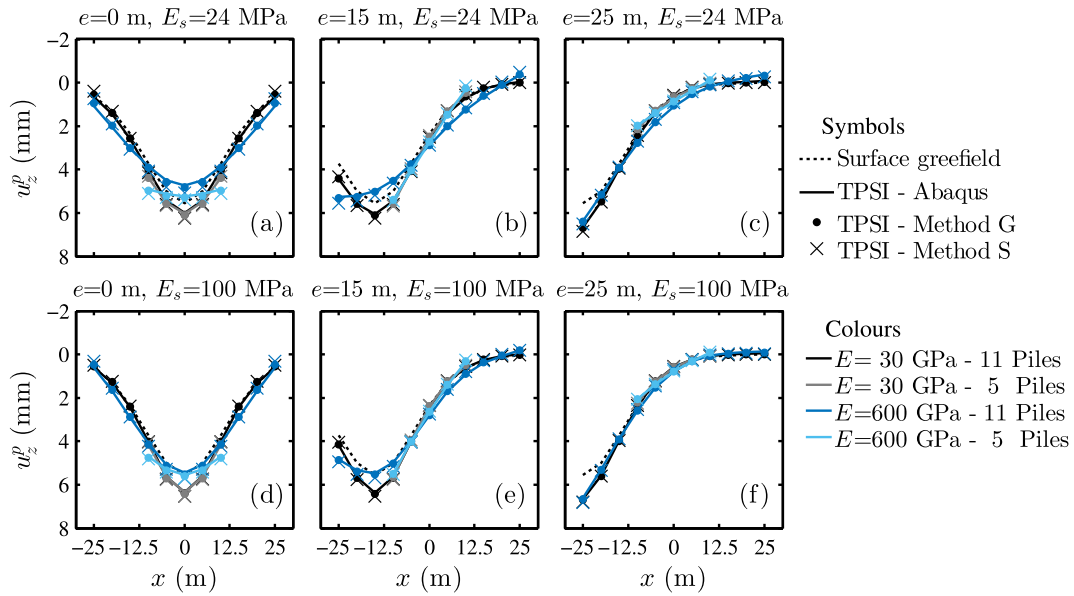


Fig. 6. Validation test results: simple beam models.

predictions was assessed using Δ_i (Eq. (14)), which is the absolute value of the ratio between the difference in pile settlement estimation with the ABAQUS and the Winkler models and the maximum surface greenfield settlement of the pile group. Fig. 7 shows that the accuracy is good for method G and acceptable for the simplified method S.

$$\Delta_i = \left| \frac{u_{p,z=0}^{Winkler} - u_{p,z=0}^{Abaqus}}{s_{z,z=0}^{max}} \right| \quad (14)$$

Particularly interesting is the settlement profile for the more flexible beam in Fig. 6(a) and (d) ($E = 30$ GPa and 11 pile foundation). The data show that piles with their tips above the tunnel (i.e. within a horizontal offset less than a tunnel radius, R , from the tunnel centreline) settle more than the greenfield ground surface, whereas piles with their tips outside this area settle by approximately the same amount as the greenfield surface, despite the presence of the superstructure. These results fit well with the defined influence zones relating pile response to surface greenfield displacements around a tunnel (see Fig. 1).

The data illustrate that the superstructure stiffness tends to reduce the maximum relative deflection of the piled structure, where the relative deflection is the distance between the settlement curve and a segment connecting two points of the curve.

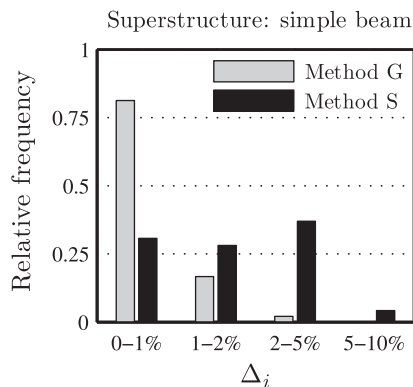


Fig. 7. Difference in pile settlement prediction, Δ_i , for simple beams.

For instance, in Fig. 6(b), the settlement of the 5-pile building varies almost linearly with transverse distance, giving near-zero values of relative deflection. Moreover, as expected, the superstructure shows more flexible behaviour when the ratio between soil and structure Young's modulus and/or the ratio between structure width and tunnel depth is high.

4.3.2. Framed structure model

A framed structure with isolated ground level columns was chosen for the validation analysis in order to emphasise effects induced by horizontal translations and rotations of the pile heads. This provides further information on the effect of structural configuration to the overall response.

Fig. 8 compares displacements and rotations of the frame structure model foundation from the Winkler-based and ABAQUS models; surface greenfield data are also included for comparison, when possible. Method S only accounts for the vertical dofs of piles; thus its use is only appropriate for the assessment of induced settlements. Displacements and rotations obtained from the tunnel-pile group interaction (TPI) analysis with a free-pile head condition are also provided in Fig. 8 to highlight the effect of the frame. The data show good agreement between the ABAQUS results and both method G (u_z^p, u_x^p, φ^p) and method S (u_z^p) predictions. The tunnel-pile interaction analysis again highlights that the piles with their tips directly above the tunnel settle more than the greenfield surface settlements, whereas piles outside this area settle slightly less than the greenfield surface displacements. The reduction of vertical settlements due to the frame stiffness, in this case, is marginal. Furthermore, the shape of the structural settlement trough (i.e. curvature profile) is not altered by the framed building. Horizontal pile head displacements due to tunnel-pile interaction agree in magnitude and distribution with the greenfield values. Horizontal ground movements are transferred to the buildings by the piled foundation and, in the TPSI analysis, frame stiffness is able to reduce the magnitude compared to the TPI displacement curve. Furthermore, rotation distributions estimated in the case of TPI and TPSI differ. Interestingly, despite the connection condition of fixed pile heads, the TPSI pile head rotation distribution is qualitatively opposite to the first derivative of the frame settlement curve for $e = 0$. This aspect and additional influences of the structural configuration are investigated further in the following section; the

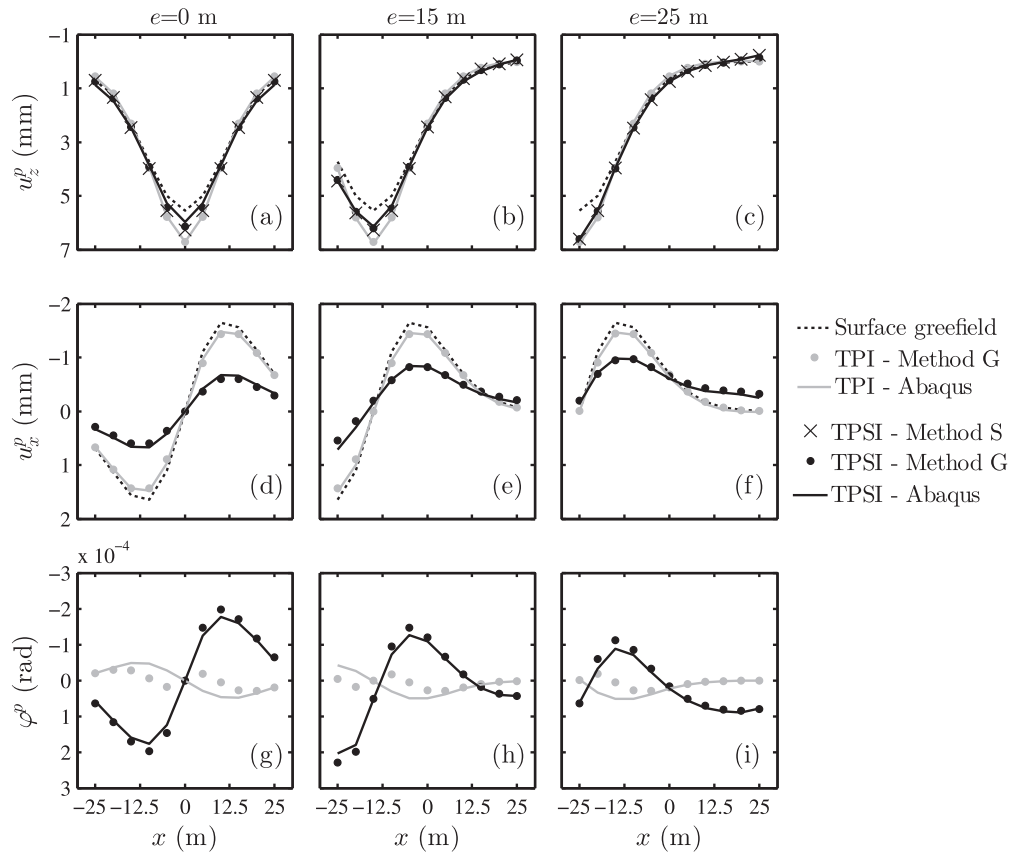


Fig. 8. Validation analysis outcomes: framed structure case.

focus of this section was to illustrate how the results Winkler-based models compare against the more rigorous ABAQUS model results.

5. Structural configuration and pile-structure connection

In this section, results from the ‘General Method’ of tunnel-pile-structure interaction analysis (TPSI-G) are used to evaluate the influence that structural configuration and pile-structure connection detail have on building displacements. Two building models were analysed: (1) a simple beam and (2) a frame. The parameters adopted for the analyses are summarised in Table 1 and results are presented in Fig. 9. For comparison, greenfield displacements are also plotted. To allow for comparison of results, a unique geotechnical domain (i.e. tunnel, soil, and foundation properties) was assumed. In addition, the two building models were given properties such that maximum settlements obtained in the tunnel-pile-structure interaction analyses were equivalent (i.e. the two buildings models had a similar stiffness). Both fixed-head (FH) and hinged-head (HH) pile-structure connections were implemented.

Note that pile head rotations have no effect on building deformations and internal forces for hinged pile-structure connections.

An important distinction between simple beams and framed buildings of similar stiffness is that, for the simple beams, the structural bending stiffness is concentrated at the ground level, whereas for frames, it is distributed over several storeys through the action of the columns. This significantly affects pile head movements and rotations resulting from tunnel-pile-structure interaction.

As illustrated in Fig. 9(a)–(c), the shape of the framed building settlement curves is similar to that of the TPI curves (i.e. tunnel-pile interaction with no structure included). On the contrary, the stiffness of simple beams tends to have a more significant effect on the settlement curve shape and the resulting width of the building in the sagging and hogging zones, B_{sag} and B_{hog} , respectively. To illustrate the modification of B_{sag} and B_{hog} , the position of the inflection point of the settlement curves in Fig. 9 are shown in Table 2. For the case $e = 0$, the inflection point offset (and therefore magnitude of B_{sag}) is increased, compared to the settlement curve resulting from TPI, more for the beam models than for the frame models.

Table 1 Model parameters - effect of structural configuration and pile-structure connection.

Tunnel		Foundation and soil		Structure		Beam	Frame		
z_t	(m)	20	E_s	(MPa)	24	E	(GPa)	30	30
R	(m)	3	ν_s	(-)	0.5	B	(m)	50	50
V_{lit}	(%)	1	E_p	(GPa)	30	# storeys	/	/	15
e	(m)	0; 15; 25	d_p	(m)	0.5	h	(m)	/	3
			L_p	(m)	15	$b_c \times d_c$	(m)	/	0.5×0.5
			s_p	(m)	5	$b_b \times d_b$	(m)	/	0.5×0.8
			# piles		11	$b_{bg} \times d_{bg}$	(m)	0.5×4	/

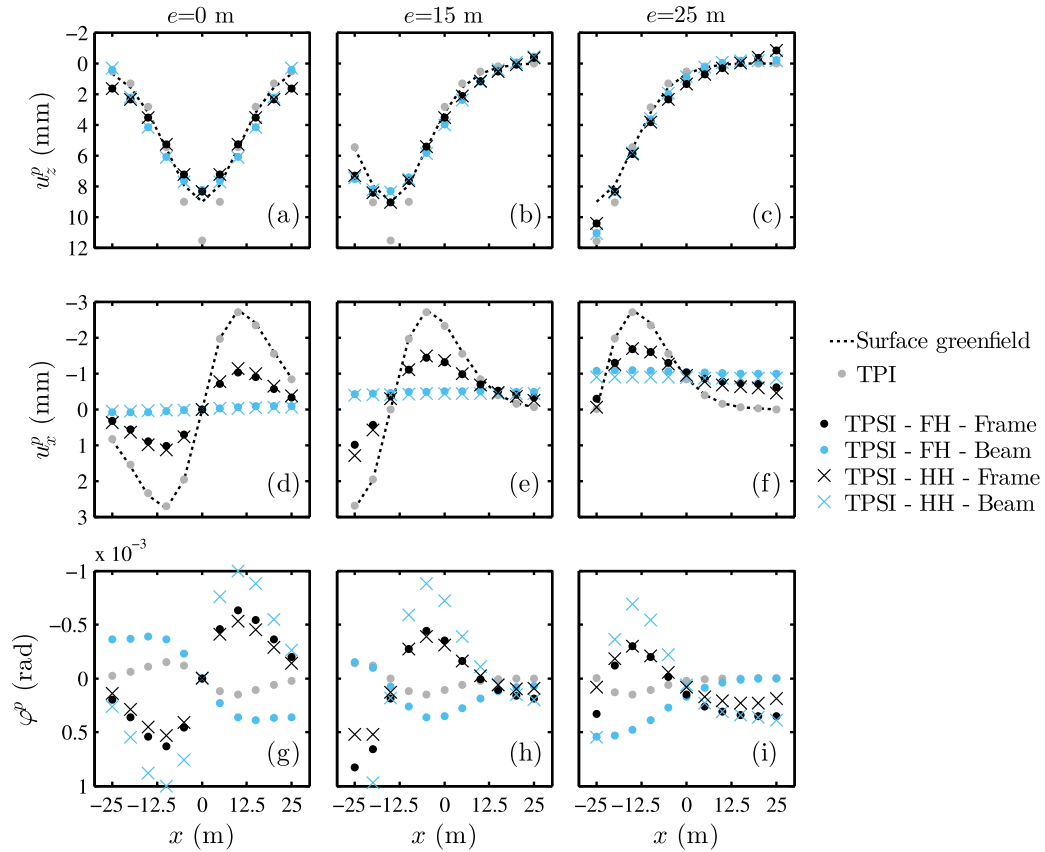


Fig. 9. Effect of structural configuration on tunnelling-induced distortions.

Table 2

Horizontal offset to inflection point, x_i , of the settlement curves in Fig. 9(a)–(c).

Case	$e = 0$ m	$e = 15$ m	$e = 25$ m
GF	±9.4	−5.6	−15.6
TPI	±6.2	−8.8	−17.2
TPSI-FH-Frame	±8.2	−7	−17.2; 15.2
TPSI-HH-Frame	±8.2	−7	−17.2; 15.2
TPSI-FH-Beam	±12	−3	−
TPSI-HH-Beam	±12	−3	−

For the case of $e = 25$ m, the settlement curve of the simple beam does not have an inflection point at all, indicating that the entire building is in hogging (i.e. $B_{hog} = B$).

The structural configuration also affects horizontal foundation movements at the surface. As shown by Fig. 9(d)–(f), the axial stiffness of the simple beam results in negligible horizontal pile head translations, whereas the framed structure is not able to prevent these movements. The horizontal movements obtained with the TPSI analysis is a reduced version of the displacements resulting from the TPI analysis. The frame resists differential pile head horizontal displacements through the bending stiffness of the base columns, which is less effective than the axial stiffness of horizontal structural elements connecting the pile heads in the beam analysis. Interestingly, the moderating effect of the structure on pile head horizontal translations induces an overall building shift towards the tunnel centreline.

Finally, the understanding of pile head rotations, ϕ^p , requires consideration of two aspects: (1) the degree of fixity of the pile heads, provided by the overall superstructure bending stiffness at the ground level and the pile-structure connections (FH or HH);

and (2) the ability of the superstructure to resist any differential horizontal movements of the foundation at the ground surface. When the frame is centred above the tunnel, TPSI analysis pile head rotation distributions are qualitatively opposite to the first derivative of the frame settlement curve (see Fig. 9(a) and (g) and note that a positive pile head rotation is anticlockwise). Pile-structure connection type (hinged or fixed) has only a marginal influence on results for this case. This happens because ground level columns, which have relatively low bending stiffness, resist differential horizontal movements between piles (i.e. drag pile heads horizontally) resulting in pile head rotations. On the other hand, for a simple beam, there is a remarkable difference in the rotations induced by hinged and fixed pile-structure connections. When the pile heads are fixed to the beam, the rotation distribution has to follow the first derivative of the settlement curve in Fig. 9(a) because of the high degree of fixity at the pile heads provided by the beam bending stiffness. For hinged pile heads, relative pile-beam rotations are allowed and the rotation curve shape is similar to that induced by a frame but with higher maximum values because the simple beam is more efficient at reducing horizontal differential movements. Similar interaction mechanisms for pile head rotation are observed when the tunnel is not centred below the building (Fig. 9(h) and (i)).

Overall, the results shown in Fig. 9 illustrate that the choice of the structural model can have an important effect on results in a tunnel-pile-building interaction analysis.

6. Deflection ratio and horizontal strain modification factors

To put results in the context of the limiting tensile strain framework, this section presents a study of the effects of relative

building stiffness on deflection ratio and horizontal strain reduction factors. A parametric study was carried out for both simple beams and framed structures considering several structural configurations, foundation detail (number and length of piles) and building eccentricities. The two-stage analysis Winkler-based method G was used. For each analysis, the computation of the deflection ratios and horizontal strains was performed using greenfield settlements and vertical displacements of the structures at the pile head locations. Horizontal strains were obtained by normalising differential horizontal displacements between two consecutive locations by their relative distance. For the calculation of the building distortions, Mair et al. (1996) suggested that the considered length of the building should be limited to the practical extent of the settlement trough, which is approximately equal to $2.5i$. The offset of the inflection point at the surface, i , was estimated using $i/R = 1.15(z_t/2R)^{0.9}$, as suggested by Loganathan and Poulos (1998). This criterion was added to the analyses performed to assess the greenfield and building distortions as well as the modification factors. The results for the framed structures are compared with simple beams using a newly proposed method for determination of relative bending and axial stiffness that accounts for the structural configuration and pile geometrical distribution beneath the building (detailed in the following section). Tables 3–5 indicate the range of parameters and structural configurations assumed for the parametric analyses. The previous section (see Fig. 9), illustrated the importance of pile-structure connections on the global tunnel-pile-structure interaction for simple beams. Therefore, the analyses of the simple beams were performed for two cases: hinged (HH) and fixed (FH) pile head. Frames were only analysed for fixed pile-structure connections because of the secondary role that the rotational restraint has on the global interaction (see Fig. 9).

6.1. Deflection ratio and relative bending stiffness

6.1.1. New relative bending stiffness parameters for piled structures

For piled foundations, it is not possible to simplify the problem to a plain strain condition. In order to define a suitable relative bending stiffness factor, the problem of a structure on a single pile row foundation is first considered (see Fig. 10(a)). For a single transverse pile row the entire superstructure contributes to the stiffening of the soil-foundation system, leading to the necessity to consider EI rather than EI^* (per m run) as defined by Franzius et al. (2006) and Farrell (2010). Therefore, in these cases, the use of the following relative bending stiffness parameters are more appropriate:

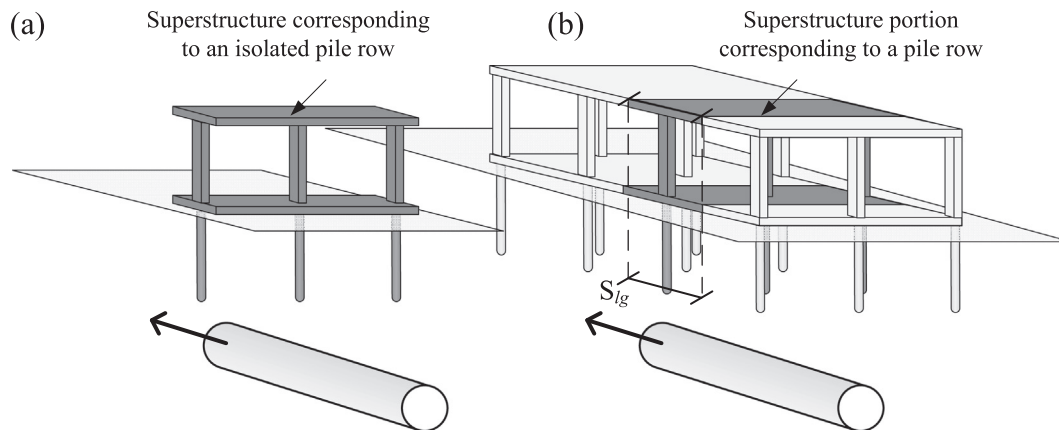


Fig. 10. Simplified approach to reduce $m \times n$ piled foundation problem to a single pile row.

$$\rho_{sag}^r = \frac{EI}{E_s B_{sag}^3} \quad \parallel \quad \rho_{hog}^r = \frac{EI}{E_s B_{hog}^3} \quad [\text{m}] \quad (15)$$

This relative stiffness parameter ρ^r , where the superscript r denotes a single pile row, has dimension of length. It is not possible to use a dimensionless term for this problem because a superstructure of finite longitudinal length interacts with the soil only through the pile row that is discrete along the longitudinal tunnel direction.

On the other hand, pile foundations are generally composed of multiple transverse pile rows. In these cases, the analysis may be simplified to that of a single pile row beneath a portion of a building or an equivalent frame. For instance, the building may be separated into independent portions corresponding to each transverse pile row (see Fig. 10(b)). This simplification is sensible when only the final building transverse deformation profile is considered (i.e. when the tunnel has passed the location of the building). By multiplying the expressions shown in Eq. (4) by the ratio between longitudinal spacing of transverse pile rows, S_{lg} , and building longitudinal length, L , the following definitions of relative bending stiffness of buildings with multiple pile rows are obtained

$$\rho_{sag}^p = \frac{EI}{E_s B_{sag}^3} \frac{S_{lg}}{L} \quad \parallel \quad \rho_{hog}^p = \frac{EI}{E_s B_{hog}^3} \frac{S_{lg}}{L} \quad [\text{m}] \quad (16)$$

where $EI(S_{lg}/L)$ is the bending stiffness of the superstructure portion corresponding to the considered transverse pile row (in kN m^2). This approach permits a direct comparison of ρ for shallow foundations to ρ^p for pile foundations. By definition, the relative stiffnesses may be evaluated from

$$\rho_{sag} = \frac{\rho_{sag}^{p,r}}{S_{lg}} \quad \parallel \quad \rho_{hog} = \frac{\rho_{hog}^{p,r}}{S_{lg}} \quad (17)$$

This definition will be used in a subsequent section to relate design charts proposed for buildings on shallow foundations to the outcomes of the tunnel-pile-structure interaction analyses presented here. Moreover, to facilitate the description of the results, the terms primary and secondary deformation modes are used as follows: for low eccentricity cases, primary = sagging and secondary = hogging; for high eccentricity cases, primary = hogging and secondary = sagging.

6.1.2. Deflection ratio of simple beam and frame models

The deflection ratio modification factors calculated from the parametric study results, M^{DR} (Eq. (1)), are plotted against the relative bending stiffness in Figs. 11 and 12. Because the analyses are performed for a single pile row, relative bending stiffness is

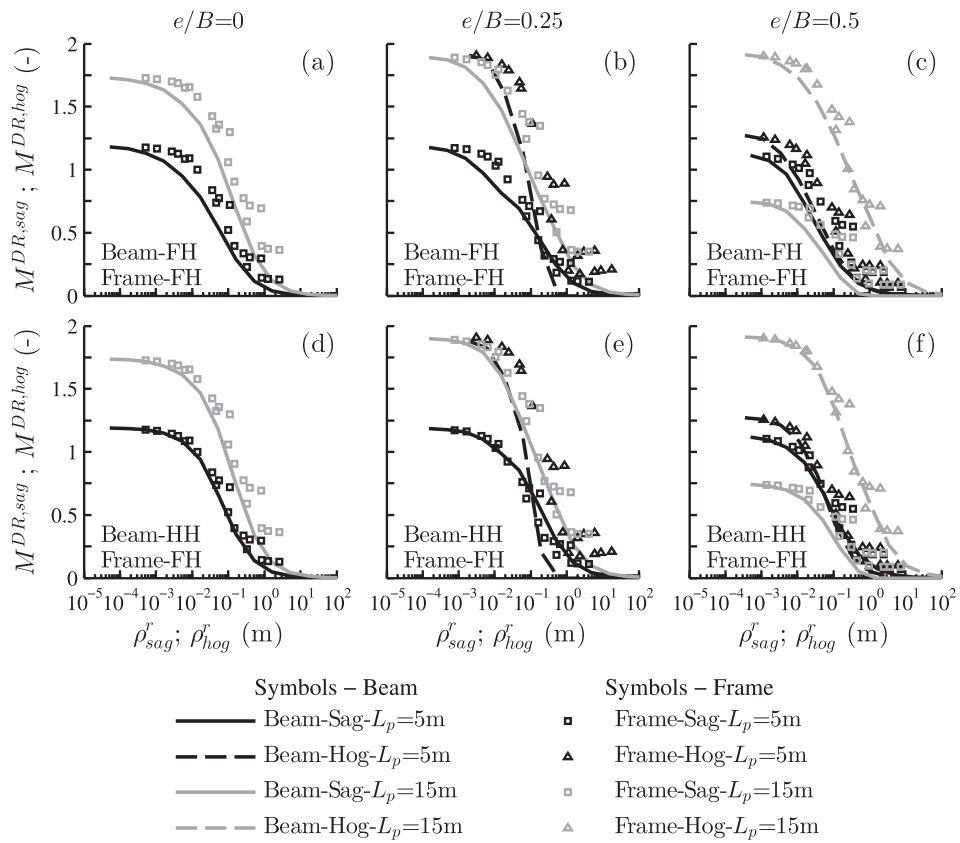


Fig. 11. Effects of building stiffness on M^{DR} for $E_s = 24$ MPa and $B = 20$ m.

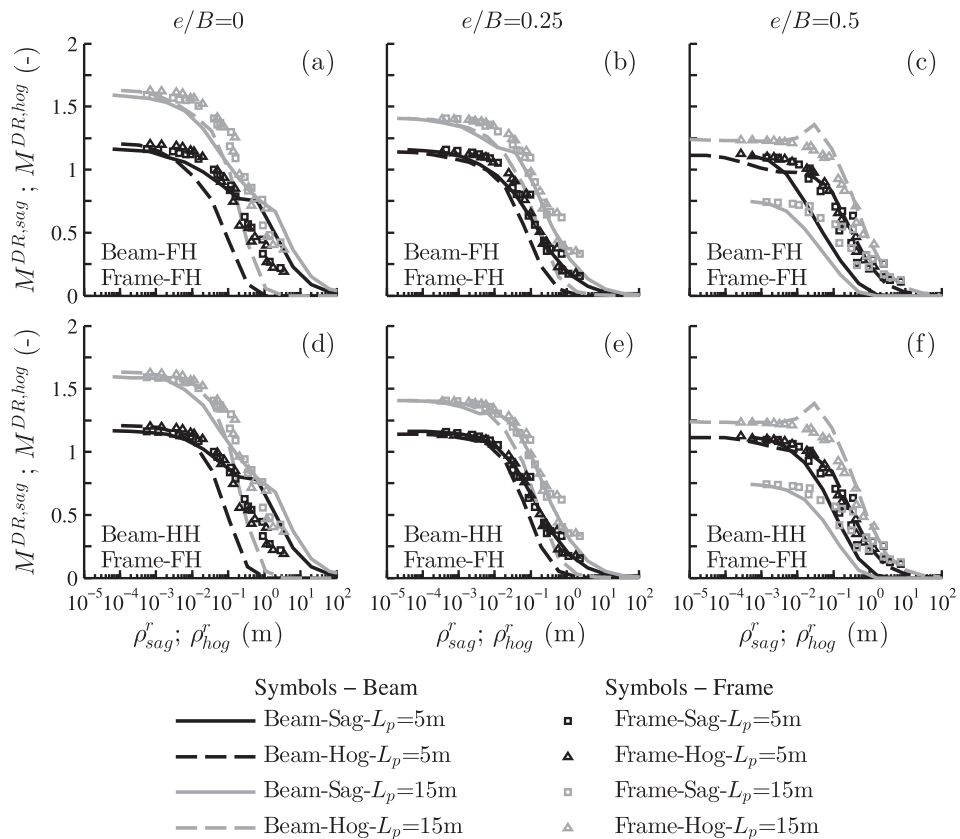


Fig. 12. Effects of building stiffness on M^{DR} for $E_s = 24$ MPa and $B = 50$ m.

described in terms of ρ^r , defined in Eq. (15), rather than ρ^p . Figs. 11 and 12 present the results for a building with a transverse width $B = 20$ and 50 m, respectively. In each case, two pile lengths, $L_p = 5; 15$ m, corresponding to relatively short and long piles with respect to the tunnel depth ($L_p/z_t = 0.25; 0.75$) were implemented and three normalised eccentricities were considered ($e/B = 0; 0.25; 0.5$). In these analyses, the building deformation mode is primarily sagging for $e/B = 0$ whereas it is mainly hogging for $e/B = 0.5$. In order to demonstrate the effectiveness of the column stiffening factor (Eq. (5)) in predicting the frame equivalent bending stiffness, Eq. (6) was used to estimate EI of the framed structures and results from the frame analyses are plotted together with those from simple beam analyses. Modification factors of frames are plotted as points whereas those of simple beams are represented with a curve. Finally, the upper charts display the variation in M^{DR} for hinged pile-simple beam connections (HH) whereas the lower charts refer to fixed pile-simple beam connections (FH). Frames are only analysed for fixed pile-structure connections (FH) because, as shown in the validation section, pile-structure connections have secondary effects on the response of framed buildings.

Figs. 11 and 12 illustrate that reduction factors are highly dependent on building eccentricity, e/B . Another important parameter is the relative pile length, L_p/z_t ; data show a marked rise of M^{DR} for a given case with an increase of L_p/z_t in both primary and secondary deformation modes (e.g. Figs. 11 and 12(a) and (d)), except for the secondary sagging deformations at high normalised eccentricity $e/B = 0.5$ (see Figs. 11 and 12(c) and (f)). Therefore, relatively long piles represent a greater potential for building damage in this context.

Furthermore, in both Figs. 11 and 12, the modification factor trends reveal qualitative differences between the case of simple beams and framed buildings. Framed buildings undergo a gradual reduction of M^{DR} with relative bending stiffness in both hogging and sagging zones; on the contrary, in the case of simple beams with both fixed and hinged pile connections, the charts show that the structural deformation follows a more complex pattern, which is due to the structural continuity of the building, preventing it from responding independently in the hogging and sagging zones. For instance, in the case of a central tunnel ($e/B = 0$) and building width $B = 50$ m (see Fig. 12(a) and (d)) hogging and sagging curves show complex and interrelated trends. After an initial decrease of both reduction factors, at approximately $\rho^r = 10^{-1}$ m, there is a sharp drop of the hogging curve whereas the sagging one remains steady up to $\rho^r = 10^0$ m. When the hogging reduction factor reaches a value close to zero, which means that the structure is undergoing a fully sagging deformation mode, any increase in structural bending stiffness contributes to further reduce the sagging reduction factor. Fig. 12 demonstrates that, for simple beams in both sagging and hogging greenfield zones, the structural stiffness is more efficient in the reduction of the secondary deformation mode (the hogging DR for low eccentricity buildings and the sagging DR for high eccentricity buildings). This outcome agrees with the results of centrifuge and numerical modelling analyses performed by Franzius et al. (2006) and Farrell et al. (2014), who studied the deformation induced by tunnelling on simple shells and plates, respectively. On the other hand, this may not be true for framed structures that, in this study, show a gradual reduction of DR in both deformation zones with the increase of relative stiffness. In general, although the relative stiffness ρ^r accounts indirectly for the tunnel location through B_{sag} and B_{hog} , detailed design charts should be a function of e/B and structural configuration.

Additionally, comparison of results for frames and simple beams illustrates the importance of the pile-structure connection

condition. For both sagging and hogging deformation modes, when beams are fixed to the pile heads (FH), most modification factors of the frames are higher than the respective curves for simple beam models (i.e. simple beams have a stiffer response than frames). When hinged connections (HH) are adopted for the simple beams, the difference reduces and results of both structural configurations show a fair agreement (as long as the reduction trends do not diverge due to the structural configuration). These results suggest that the structural scheme based on simple beams pinned to the pile heads is the most suitable to be used as an equivalent structure for piled framed buildings without horizontal structural elements at the ground level, although a different building response to tunnelling should still be expected. This occurs because frames without a stiff raft are not able to provide a high level of bending resistance at the pile heads. Secondly, fixed pile-structure connections contribute more than hinged connections to the stiffening effect of the superstructure; this is because the bending stiffness of the piles contributes to the resistance against building deformation, whereas for hinged connections there would not be this stiffening contribution of the pile foundation.

6.2. Horizontal strains and relative axial stiffness

Because of the capability of piles to mobilise horizontal movements, simple beams and framed buildings with piled foundations may undergo significant horizontal strains. This section investigates the effects of structural configuration and pile-structure connections on horizontal strain modification factors, M^e , defined by Eq. (2), and introduces a unique dimensionless axial stiffness parameter for both simple beams and frame buildings. As for the analysis of relative bending stiffness, the case of a structure on a single pile row is considered. When the building has multiple transverse pile rows, it is necessary to distribute the building stiffness between the pile rows, as shown in Fig. 10(b), in order to consider the appropriate portion of the building. To account for the axial stiffness of either a simple beam or a horizontal structural element connecting pile heads in framed buildings, the structural scheme shown in Fig. 13 was considered. This consists of a portal with a beam at the ground level connecting two pin-supports. The axial stiffness of this beam is referred to as EA_{bg} . As shown in the validation section, for piled foundations, the pile-structure connection has a negligible effect on horizontal movements and therefore strains. As a result, the conservative structural scheme based on pin-supports may be considered to be representative. Similar to Goh and Mair (2014), the frame stiffness factor, α_f , is defined by imposing a unit differential horizontal displacement, Δ , between the pin-supports and calculating the external horizontal reaction force, H' , resulting in

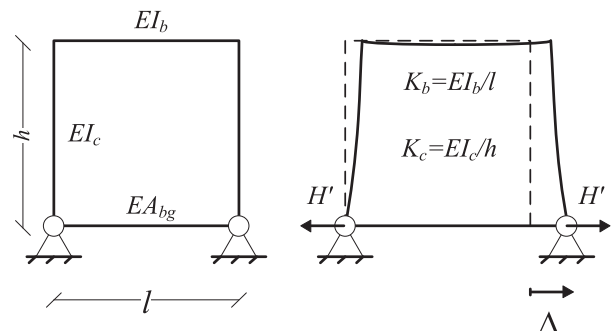


Fig. 13. Portal response analysis to a differential horizontal displacement of the supports.

Table 3
Investigation of modification factors: combination of stiffness for simple beams.

Simple beam (15 cases)			Min	Max
Bending stiffness	EI	(kN m ²)	10 ⁴	10 ¹¹
Axial stiffness	EA	(kN)	10 ⁴	10 ¹¹

Table 4
Investigation of modification factors: soil, tunnel and foundation parameters and configurations.

Tunnel			Foundation and soil		
z_t	(m)	20	E_s	(MPa)	24
R	(m)	3	ν_s	(-)	0.5
V_{lt}	(%)	1	E_p	(GPa)	30
e/B	0; 0.25; 0.5		d_p	(m)	0.5
			L_p	(m)	5; 15
			s_p	(m)	5
			# piles		5; 11

Table 5
Investigation of modification factors: framed structure configurations.

Structure	A	B	C	D	
E	(GPa)	30	30	30	30
# storeys		2; 4; 10; 15; 30			
h	(m)	3	3	3	3
l	(m)	5	5	5	5
$b_c \times d_c$	(m)	0.2 × 0.2	0.3 × 0.3	0.5 × 0.5	0.7 × 0.7
$b_b \times d_b$	(m)	0.2 × 0.2	0.3 × 0.5	0.5 × 0.8	0.7 × 1.0
$b_{bg} \times d_{bg}$	(m)	Absent			

$$\alpha_f = \frac{H'}{\Delta} = \frac{3K_b K_c}{h^2(2K_b + 3K_c)} + \frac{EA_{bg}}{l} \quad [\text{kN/m}] \quad (18)$$

The first term of α_f represents the contribution of the portal to the overall axial stiffness of the building at the ground level whereas the latter relates to the contribution of a simple beam. To account for the soil stiffness, it would be appropriate to define the relative axial stiffness as

$$\alpha_f^* = \frac{1}{E_s} \left[\frac{3K_b K_c}{h^2(2K_b + 3K_c)} + \frac{EA_{bg}}{l} \right] \quad [\text{m}] \quad (19)$$

Interestingly, the second term of this expression is similar to $\alpha_{mod}^* = EA/(E_s BL)$ (Eq. (3)), with the bay length l instead of the building width B and the longitudinal building length L omitted (which is sensible considering that the soil interacts with the piles and not directly with the entire superstructure).

The cases presented in Tables 3–5 were also used for this analysis. Fig. 14 plots, for both beams and frames, the calculated values of M^{eh} against α_f^* , defined using Eq. (19). Results illustrate that horizontal strain reduction factors are not affected by the pile length, L_p , but are influenced by building transverse width, B , and building normalised eccentricity, e/B . Moreover, Fig. 14 indicates three notable points. Firstly, the distribution of the results demonstrates the efficiency of horizontal ground level structural elements to reduce horizontal strains (for the given soil-pile foundation system, a wide range of simple beams are able to achieve a value of $M^{eh} = 0$, whereas the stiffest frames are only able to reduce M^{eh} to 0.4). Secondly, despite the similar trend of results for simple beams and frames, most results from the frames are below those of the simple beams; this may be due to the assumed simplified

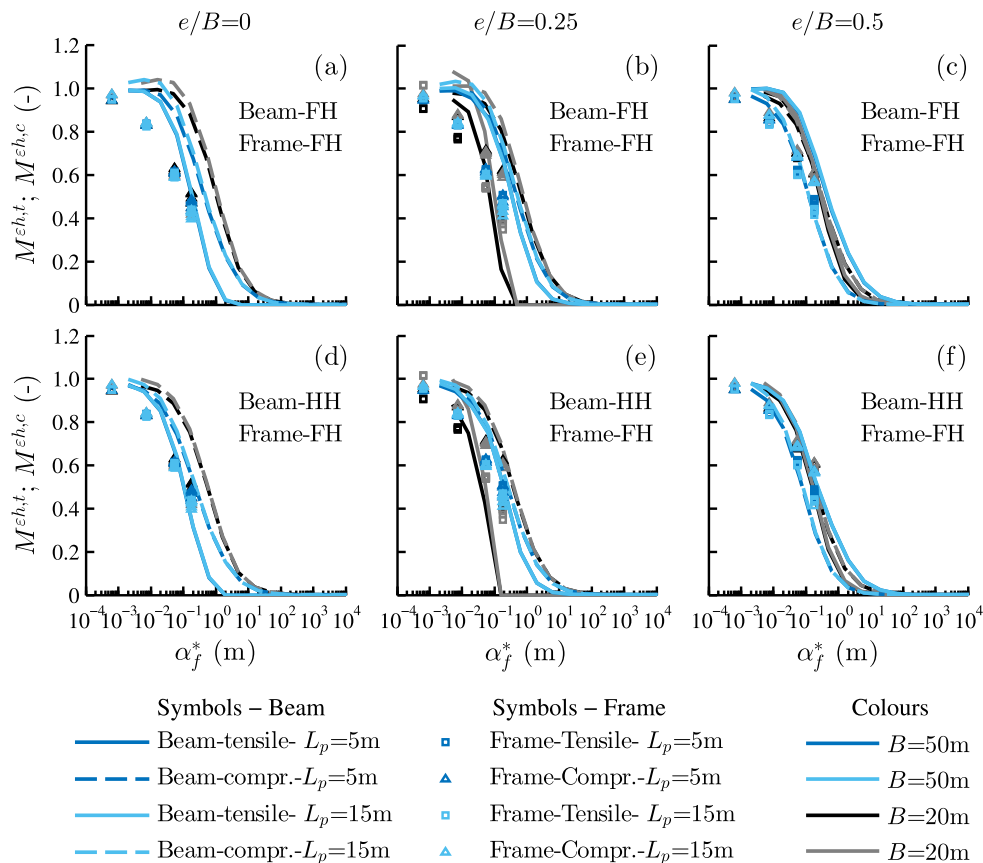


Fig. 14. Effects of building stiffness on M^{eh} for $E_s = 24$ MPa and $B = 20, 50$ m.

Table 6
Parameters and configurations for the parametric study.

Tunnel			Foundation and soil		
z_t	(m)	20	E_s	(MPa)	5; 25; 100
R	(m)	3	ν_s	(-)	0.5
$V_{i,t}$	(%)	1	E_p	(GPa)	30
e/B	0; 0.25; 0.5		d_p	(m)	0.5; 1
			L_p	(m)	5; 15
			s_p	(m)	5; 10
			# piles		5; 10; 25

structural scheme that consists of a single-span one-storey portal, which neglects the frame complexity. The α_f^* term does not accurately account for the structural configuration; the design charts proposed in the following section are therefore a function of the structural configuration. Finally, the minor effects of pile head connection (hinged or fixed) to the superstructure, discussed in the previous section, is once again confirmed (by comparing results in Fig. 14(a)–(c) with results in Fig. 14(d)–(f)). However, in general, for simple beam structures, at a given relative axial stiffness, the reduction factors M^{eh} are slightly higher for the fixed pile-structure condition than for the hinged connection.

6.3. Proposed envelopes for modification factors

An additional extensive parametric analysis was conducted to provide design charts for estimation of the modification factors due to tunnelling beneath piles. Attention was focused on the geotechnical domain by considering a wide range of parameters for the piled foundations and the soil; Table 6 summarises the considered soil-pile foundation configurations. The superstructure properties, both simple beams and frames, were defined as in the previous section (see Tables 3 and 5). Only fixed pile-structure connections were implemented. The relative bending stiffness ρ^r and the relative axial stiffness α_f^* indicated in Eqs. (15) and (19) were adopted. Because the tunnel-building eccentricity influences the modification factors, results for different values of e/B are

distinguished in the proposed charts with different marks. The proposed envelopes may be useful for engineers to conduct a preliminary risk assessment.

6.3.1. Deflection ratio modification factors

The results of M^{DR} from the full parametric study are plotted in Fig. 15 against ρ^r , which is equivalent to $S_{lg}\rho$ (Eq. (17)). Included in the figure is a proposed upper and lower design envelope. Reduction factors associated with an absolute value of DR_{gf} lower than $2 \cdot 10^{-3}\%$ were omitted because they do not have potential for damage and the ratio M obtained with a small denominator should not be considered representative. The results in sagging and hogging regions are provided in the left and right plots of the figure, respectively. To highlight the influence of relative pile length L_p/z_t on the global interaction, results are distinguished between relatively short and long piles. Considering the relative bending stiffness of the building, the outcomes suggest that for piled structures, a fully flexible response is expected up to about $\rho^r = 10^{-3} - 10^{-2}$ m, depending on relative pile length (Fig. 15). Note that the values of the upper and lower envelopes begin to decrease for $\rho^r > 10^{-2}$ m. This indicates that performing a tunnel-pile interaction analysis, which neglects the contribution of the structure, may be overly conservative when $\rho^r > 10^{-2}$ m. Buildings start to experience negligible deformations (i.e. a fully rigid response) within the range of about $\rho^r = 10^0 - 10^2$ m. At a given relative building stiffness, buildings on relatively long piles are more likely to undergo higher deflection ratios than buildings on short piles. Generally, the increase of M^{DR} with L_p/z_t is due to subsurface movements having a greater effect. However, this does not apply to the estimation of $M^{DR,sag}$ in the case of relatively long piles where $e/B = 0.5$ (see Fig. 15(a) where values of $M^{DR,sag}$ fall below the lower envelope). The presence of these outliers is probably due to the efficiency of simple beams to reduce deformations due to the secondary deformation mode.

To highlight the effect of piles, the envelopes suggested by Mair (2013) for shallow foundations are also plotted in Fig. 15 considering $\rho^r = S_{lg}\rho$ and assuming a longitudinal spacing between pile

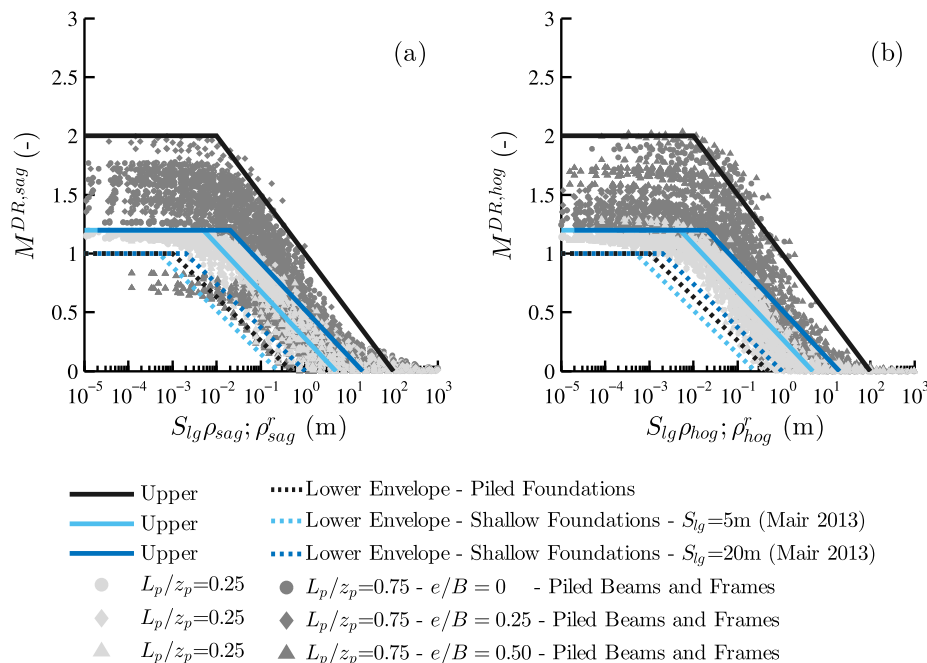


Fig. 15. Proposed envelopes for the estimation of M^{DR} for piled foundations.

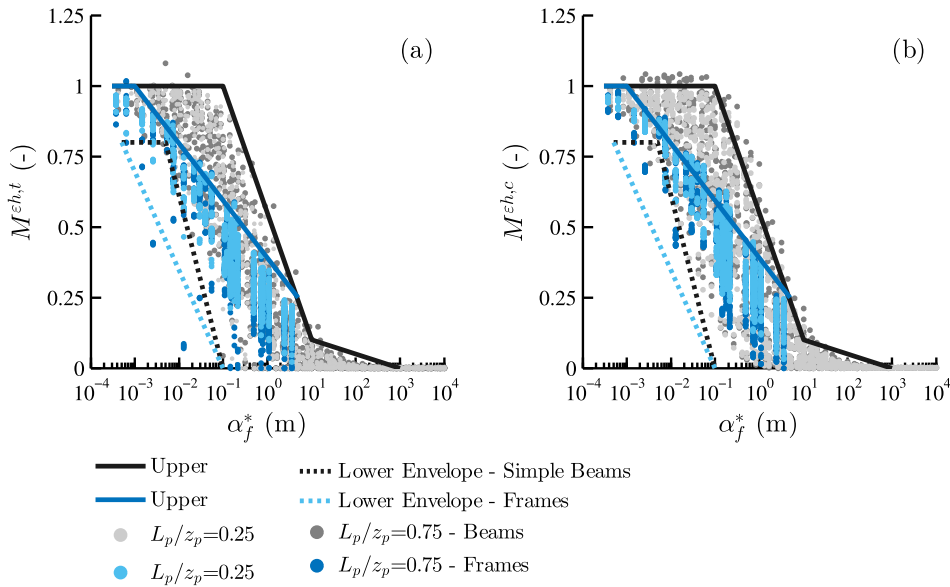


Fig. 16. Proposed envelopes for the estimation of M^{eh} for piled foundations.

rows of $S_{lg} = 5$ and 20 m to cover a realistic range of pile spacing. In the chart, the magnitude of the envelope translation due to S_{lg} is minor because of the logarithmic scale of the x-axis. The proposed lower envelope is comparable to that obtained by Mair (2013) for shallow foundations; this is probably due to the fact that relatively short piles are mostly affected by the distributions of surface greenfield movements, similar to the case of buildings on rafts and footings. In contrast, the upper envelopes for shallow and deep foundations illustrate the considerable detrimental role played by piled foundations in tunnel-building interaction, especially for flexible structures.

6.3.2. Horizontal strain modification factors

Upper and lower envelopes of the horizontal strain modification factor, M^{eh} , are plotted in Fig. 16 together with results of the full parametric investigation. Results are distinguished between relatively short and long piles and for simple beam and frame models.

Results in Fig. 16 illustrate the secondary effect of L_p/z_t on M^{eh} . On the contrary, there is a marked difference in the reduction trends of piled beam and frame models: M^{eh} for beam models may be higher than for frames at a given relative axial stiffness. Despite this, Fig. 16 indicates the suitability of the dimensionless modification factor α_f^* in describing the building contribution to the reduction of differential horizontal displacements between pile heads for several soil and foundation configurations. To account for the structural scheme, two distinct upper envelopes are proposed for beams and frames, as shown in Fig. 16. In general, neglecting the effects of piles for fully flexible structures may be adequate because the maximum recorded value of M^{eh} was only slightly higher than unity. On the other hand, for partially flexible beams with $\alpha_f^* > 10^{-1}$ m and partially flexible frames with $\alpha_f^* > 10^{-3}$ m, reduction factors decline steadily; assuming greenfield horizontal strains would be overly conservative in these cases. A rigid building response should be expected for $\alpha_f^* > 10^3$ m.

Based on the envelopes for simple beams shown in Fig. 16, it is interesting to notice that a rigid response is observed in most practical cases of piled structures with horizontal structural elements at the ground level. For instance, a simple beam with a 0.25×0.25 m² cross-section and $E = 30$ GPa has an axial stiffness of $1.9 \cdot 10^6$ kN. If the building model consists only of these beams

and E_s and l are assumed to be 25 MPa and 5 m, respectively, the relative axial stiffness of the system is $\alpha_f^* = 1.5 \cdot 10^1$ m, which is associated with very low value of M^{eh} in Fig. 16. Therefore, horizontal ground strains transferred into a piled superstructure with continuous horizontal structural elements at the ground level would be negligible unless an unrealistically small axial stiffness is considered. On the contrary, as indicated by Goh and Mair (2014) for frames on single footings, in the case of piled frame structures without ground level strips or rafts, differential horizontal movements between pile heads are expected, which may induce damage in non-structural elements, such as infill walls, or to the ground floor columns. However, horizontal strains should be negligible at the first floor level (i.e. at the top of the ground level columns) because of the constraint provided by the axial stiffness of the first-floor beam/slab.

7. Conclusions

A study of the tunnel-piled building interaction has been presented in this paper based on elastic Winkler-based Two-Stage Analysis Methods (TSAMs). Analyses were limited to the case of tunnelling beneath piled elastic frame structures or simple equivalent beams. Results for varying levels of soil and structural stiffness, structural configuration, and relative foundation-tunnel location compared well with results from 3D FEM numerical models. The Winkler-based TSAMs allow for a remarkable reduction of the computational cost compared to 3D FEM analyses and represent a reliable and versatile tool for parametric studies. The proposed analysis approach allows for a detailed structural analysis that can evaluate the deformations of each member of the superstructure (i.e. beams and columns). This results in a more detailed damage assessment compared to a preliminary analysis based on the limiting tensile strain method, which only evaluates the overall degree of damage within the building.

Extensive parametric analyses highlighted the role of tunnel-pile interaction and the superstructure in the global tunnel-soil-building system response. Design charts were developed as a practical guidance to estimate deflection ratio and horizontal strain modification factors depending on relative bending and axial stiffness, respectively. New bending and axial relative stiffness factors were proposed to account for the presence of the

piles and allow comparison of frame axial stiffness to that of simple beams. The following conclusions can be drawn from the results provided in the paper.

- Vertical settlements are mainly induced by tunnel excavations beneath piled structures. The stiffness of buildings has a significant effect on the pile settlements and the resulting building deflections; assuming that the building as a fully flexible structure (i.e. performing a tunnel-pile interaction analysis) can be overly conservative. Tunnelling-induced horizontal strains in the superstructure are negligible in the case of a continuous foundation at the ground level (i.e. strips or raft) whereas they may be significant in framed buildings when pile heads are not connected by horizontal structural elements. In this case, the horizontal movement distribution obtained with the tunnel-pile-structure interaction analysis is a moderated version of the displacements resulting from the tunnel-pile interaction.
- The structural configuration is very important; a different response for a piled simple beam and a piled frame is expected. In particular, the structural stiffness of simple beams was found to be more efficient in reducing deformations associated with the secondary inflection mode (i.e. hogging for low eccentricity cases and sagging for high eccentricity cases). Framed structures exhibited a gradual reduction of deformations in hogging and sagging but preserved the shape of the settlement curve even for relatively stiff structures. Neither the response nor the damage of framed buildings can be fully described using a simple beam model.
- The pile-structure connection (hinged or fixed pile heads) plays an important role in tunnel-pile-structure interaction for simple beams and structures whose stiffness is concentrated at the ground level (i.e. frame structure with piled raft foundation). The pile-to-structure connection effect is secondary for framed buildings when pile heads are isolated or connected by slender elements, which is probably due to the relatively low bending stiffness of columns. Furthermore, the results of tunnel-pile-structure interaction analyses suggest that hinged pile-structure connections should be adopted in equivalent simple beam analyses of framed building with relatively low bending stiffness at the ground level.

The results provided in this paper are based on the simplifying assumptions of soil linearity and perfect bonding between the pile and soil. Therefore, this work represents a first step towards the understanding of the global tunnel-pile-structure interaction. Further investigations should be carried out to clarify the influence of ground conditions, tunnel volume loss level, superstructure weight, and tunnel head excavation advancement on the global tunnel-pile-structure interaction. However, the paper provides important insight into the problem of tunnelling beneath piled structures and contributes to the definition of the key interaction phenomena and parameters involved in the tunnel-piled building response.

Acknowledgements

This work was supported by the Engineering and Physical Sciences Research Council (EPSRC) [grant number EP/K023020/1, EPSRC Doctoral Training Award].

References

- Basile, F., 2014. Effects of tunnelling on pile foundations. *Soils Found.* 54 (3), 280–295.
- Burland, J.B., Mair, R.J., Standing, J.R., 2004. Ground performance and building response due to tunnelling. In: Jardine, R.J., Potts, D.M., Higgins, K.G. (Eds.), *Advances in Geotechnical Engineering: The Skempton Conference – Proceedings of a Three Day Conference on Advances in Geotechnical Engineering*, organised by the Institution of Civil Engineers, vol. 1. Thomas Telford Services Ltd, London, United Kingdom, pp. 291–344.
- Chen, L.T., Poulos, H.G., Loganathan, N., 1999. Pile responses caused by tunneling. *J. Geotech. Geoenviron. Eng.* 125 (2–3), 207–215.
- Devriendt, M., Williamson, M., 2011. Validation of methods for assessing tunnelling-induced settlements on piles. *Ground Eng.*, 25–30.
- Dias, T.G.S., Bezuijen, A., 2015. Data analysis of pile tunnel interaction. *J. Geotech. Geoenviron. Eng.* 141 (12), 04015051.
- Dimmock, P.S., Mair, R.J., 2008. Effect of building stiffness on tunnelling-induced ground movement. *Tunn. Undergr. Space Technol.* 23 (4), 438–450.
- Fargnoli, V., Gragnano, C.G., Amorosi, A., Boldini, D., 2015. 3D numerical modelling of soil-structure interaction during EPB tunnelling. *Géotechnique* 65 (1), 23–37.
- Farrell, R., 2010. *Tunnelling in Sands and The Response of Buildings*. Ph.D. Thesis, Cambridge University.
- Farrell, R., Mair, R., Sciotti, A., Pigorini, A., 2014. Building response to tunnelling. *Soils Found.* 54 (3), 269–279.
- Franza, A., Haji, T., Marshall, A.M., 2016. A Winkler-based method for the assessment of tunnelling-induced deformations on piled structures. In: Ni, J. C., Yang, J., Chen, S.-L., Qiu, T. (Eds.), *Proceedings of 4th Geo-China International Conference*, No. 260 GSP. American Society of Civil Engineers (ASCE), Shandong, China, pp. 259–266.
- Franza, A., Marshall, A.M., 2015. Semi-analytical prediction of ground movements due to shallow tunnels in sand. *Proceedings of the XVI ECSMGE Geotechnical Engineering for Infrastructure and Development*, vol. 2. Edinburgh, United Kingdom, pp. 461–466.
- Franzius, J.N., Potts, D.M., Burland, J.B., 2006. The response of surface structures to tunnel construction. *Proc. ICE – Geotech. Eng.* 159 (1), 3–17.
- Giardina, G., DeJong, M.J., Mair, R.J., 2015. Interaction between surface structures and tunnelling in sand: centrifuge and computational modelling. *Tunn. Undergr. Space Technol.* 50, 465–478.
- Goh, K.H., Mair, R.J., 2011. Building damage assessment for deep excavations in Singapore and the influence of building stiffness. *Geotech. Eng. J. SEAGS AGSSEA* 42 (3), 1–12.
- Goh, K.H., Mair, R.J., 2014. Response of framed buildings to excavation-induced movements. *Soils Found.* 54 (3), 250–268.
- González, C., Sagasetta, C., 2001. Patterns of soil deformations around tunnels. Application to the extension of Madrid Metro. *Comput. Geotech.* 28 (67), 445–468.
- Huang, M., Zhang, C., Li, Z., 2009. A simplified analysis method for the influence of tunnelling on grouped piles. *Tunn. Undergr. Space Technol.* 24 (4), 410–422.
- Jacobsz, S.W., Standing, J.R., Mair, R.J., Hagiwara, T., Sugiyama, T., 2004. Centrifuge modelling of tunnelling near driven piles. *Soils Found.* 44 (1), 49–56.
- Kaalberg, F.J., Teunissen, E.A.H., van Tol, A.F., Bosch, J.W., 2005. Dutch research on the impact of shield tunnelling on pile foundations. In: Bakker, K.J., Bezuijen, A., Broere, W., Kwast, E.A. (Eds.), *Proceedings of the 5th International Symposium on Geotechnical Aspects of Underground Construction in Soft Ground*. Taylor & Francis - Balkema, Amsterdam, the Netherlands, pp. 123–131.
- Kitiyodom, P., Matsumoto, T., Kawaguchi, K., 2005. A simplified analysis method for piled raft foundations subjected to ground movements induced by tunnelling. *Int. J. Numer. Anal. Meth. Geomech.* 29 (15), 1485–1507.
- Klar, A., Marshall, A.M., 2008. Shell versus beam representation of pipes in the evaluation of tunneling effects on pipelines. *Tunn. Undergr. Space Technol.* 23 (4), 431–437.
- Loganathan, N., Poulos, H.G., 1998. Analytical prediction for tunneling-induced ground movements in clays. *J. Geotech. Geoenviron. Eng.* 124 (9), 846–856.
- Loganathan, N., Poulos, H.G., Xu, K.J., 2001. Ground and pile-group responses due to tunnelling. *Soils Found.* 41 (1), 57–67.
- Losacco, N., Burghignoli, A., Callisto, L., 2014. Uncoupled evaluation of the structural damage induced by tunnelling. *Géotechnique* 64 (8), 646–656.
- Mair, R., 2013. Tunnelling and deep excavations: ground movements and their effects. In: Anagnostopoulos, A., Pachakis, M., Tsatsanifos, C. (Eds.), *Proceedings of the 15th European Conference on Soil Mechanics and Geotechnical Engineering – Geotechnics of Hard Soils – Weak Rocks (Part 4)*. IOS Press, Amsterdam, the Netherlands, pp. 39–70.
- Mair, R., Williamson, M., 2014. The influence of tunnelling and deep excavation on piled foundations. In: Yoo, C., Park, S.-W., Kim, B., Ban, H. (Eds.), *Proceedings of the 8th International Symposium on Geotechnical Aspects of Underground Construction in Soft Ground*. Taylor and Francis - Balkema, Seoul, South Korea, pp. 21–30.
- Mair, R.J., Taylor, R.N., 2001. *Elizabeth House: settlement predictions. Building Response to Tunnelling: Case Studies from Construction of the Jubilee Line Extension*, vol. 1. Thomas Telford, London, United Kingdom, pp. 195–215.
- Mair, R.J., Taylor, R.N., Burland, J.B., Taylor, R.N., 1996. Prediction of ground movements and assessment of risk of building damage due to bored tunnelling. In: Mair, R.J., Taylor, R.N. (Eds.), *Proceedings of the International Symposium on Geotechnical Aspects of Underground Construction in Soft Ground*. Balkema, Rotterdam, London, United Kingdom, pp. 713–718.
- Maleki, M., Sereshteh, H., Mousivand, M., Bayat, M., 2011. An equivalent beam model for the analysis of tunnel-building interaction. *Tunn. Undergr. Space Technol.* 26 (4), 524–533.
- Marshall, A., Mair, R., 2011. Tunneling beneath driven or jacked end-bearing piles in sand. *Can. Geotech. J.* 48 (12), 1757–1771.
- Marshall, A.M., Haji, T., 2015. An analytical study of tunnel-pile interaction. *Tunn. Undergr. Space Technol.* 45, 43–51.

- Mindlin, R.D., 1936. Force at a point in the interior of a semi-infinite solid. *J. Appl. Phys.* 7 (5), 195–202.
- Mylonakis, G., Gazetas, G., 1998. Settlement and additional internal forces of grouped piles in layered soil. *Géotechnique* 48 (1), 55–72.
- Ng, C.W.W., Lu, H., Peng, S.Y., 2012. Three-dimensional centrifuge modelling of the effects of twin tunnelling on an existing pile. *Tunn. Undergr. Space Technol.* 35, 189–199.
- Potts, D.M., Addenbrooke, T.I., 1997. A structure's influence on tunnelling-induced ground movements. *Proc. Inst. Civ. Eng.: Geotech. Eng.* 125 (2), 109–125.
- Randolph, M.F., Wroth, C.P., 1979. An analysis of the vertical deformation of pile groups. *Géotechnique* 29 (4), 423–439.
- Randolph, M.F., Wroth, P.C., 1978. Analysis of deformation of vertically loaded piles. *J. Geotech. Eng. Div.* 104 (12), 1465–1488.
- Selemetas, D., 2005. The Response of Full-scale Piles and Piled Structures to Tunnelling. Ph.D. Thesis, Cambridge University.
- Simulia, 2010. ABAQUS Analysis User's Manual. Dassault Systèmes, Providence, RI, U.S.A.
- Soomro, M.A., Hong, Y., Ng, C.W.W., Lu, H., Peng, S., 2015. Load transfer mechanism in pile group due to single tunnel advancement in stiff clay. *Tunn. Undergr. Space Technol.* 45, 63–72.
- Vesic, A.B., 1961. Bending of beams resting on isotropic elastic solid. *J. Eng. Mech. Div.* 87 (EM2, Part 1), 35–53.
- Zhang, R., Zheng, J., Pu, H., Zhang, L., 2011a. Analysis of excavation-induced responses of loaded pile foundations considering unloading effect. *Tunn. Undergr. Space Technol.* 26 (2), 320–335.
- Zhang, R.J., Zheng, J.J., Yu, S., 2013. Responses of piles subjected to excavation-induced vertical soil movement considering unloading effect and interfacial slip characteristics. *Tunn. Undergr. Space Technol.* 36, 66–79.
- Zhang, R.J., Zheng, J.J., Zhang, L.M., Pu, H.F., 2011b. An analysis method for the influence of tunneling on adjacent loaded pile groups with rigid elevated caps. *Int. J. Numer. Anal. Meth. Geomech.* 35 (18), 1949–1971.